

# *Palaeoecological potential of phytoliths from lake sediment records from the tropical lowlands of Bolivia*

Article

Accepted Version

Creative Commons: Attribution-Noncommercial-No Derivative Works 4.0

Plumpton, H. J., Mayle, F. E. ORCID: <https://orcid.org/0000-0001-9208-0519> and Whitney, B. S. (2020) Palaeoecological potential of phytoliths from lake sediment records from the tropical lowlands of Bolivia. *Review of Palaeobotany and Palynology*, 275. 104113. ISSN 0034-6667 doi: <https://doi.org/10.1016/j.revpalbo.2019.104113> Available at <https://centaur.reading.ac.uk/87043/>

It is advisable to refer to the publisher's version if you intend to cite from the work. See [Guidance on citing](#).

To link to this article DOI: <http://dx.doi.org/10.1016/j.revpalbo.2019.104113>

Publisher: Elsevier

All outputs in CentAUR are protected by Intellectual Property Rights law, including copyright law. Copyright and IPR is retained by the creators or other copyright holders. Terms and conditions for use of this material are defined in the [End User Agreement](#).

[www.reading.ac.uk/centaur](http://www.reading.ac.uk/centaur)

**CentAUR**

Central Archive at the University of Reading

Reading's research outputs online

1 Palaeoecological potential of phytoliths from lake sediment records from the tropical  
2 lowlands of Bolivia

3 Authors

4 Heather J. Plumpton<sup>a\*</sup>, Francis M. Mayle<sup>a</sup>, Bronwen S. Whitney<sup>b</sup>

5 Author affiliations

6 <sup>a</sup>School of Archaeology, Geography and Environmental Science, University of Reading, UK

7 <sup>b</sup>Department of Geography and Environmental Sciences, Northumbria University, UK

8 \*Corresponding author. Email address: [hjplumpton@gmail.com](mailto:hjplumpton@gmail.com). Postal address: Russell Building,  
9 School of Archaeology, Geography and Environmental Science, University of Reading, Whiteknights,  
10 P.O. Box 227, Reading RG6 6DW, Berkshire, UK.

11 Abstract

12 Phytolith analysis is conventionally an archaeo-botanical tool used to study past human activity using  
13 material from excavations or soil pits. However, phytolith analysis also has potential as a  
14 palaeoecological tool, to reconstruct vegetation changes through periods of climatic change and  
15 human influence. To study phytoliths from lake sediment alongside pollen requires an understanding  
16 of phytolith taphonomy in lakes. Theoretical models suggest phytoliths represent more local  
17 vegetation at smaller spatial scales than pollen from lake sediments, but this has not been tested  
18 empirically in the Neotropics. This paper compares pollen and phytolith assemblages from the same  
19 lake sediment surface sample, from a suite of lakes of different sizes across different vegetation  
20 types of lowland tropical Bolivia. We find three factors driving phytolith composition in lakes:  
21 taphonomy, lake size and phytolith productivity. By comparing phytolith assemblages with pollen  
22 assemblages, we find that they provide different taxonomic information and generally complement  
23 each other as palaeo-vegetation proxies. We also demonstrate empirically that pollen assemblages  
24 in lake samples represent a larger catchment area than phytolith assemblages. Our findings suggest

25 that phytoliths can be particularly useful in providing local-scale vegetation histories from large  
26 lakes, to complement the regional-scale vegetation histories provided by pollen data.

27

28 [Keywords](#)

29 Phytoliths, pollen, taphonomy, lake records, tropical, South America

30 [1. Introduction](#)

31 Phytolith analysis is conventionally an archaeo-botanical tool to study past human activity, used by  
32 archaeologists studying material from excavations and/or soil pits. However, phytolith analysis also  
33 has the potential, as a palaeoecological tool, to reconstruct vegetation changes through periods of  
34 climatic change and/or human influence. There are two key areas where phytoliths can provide  
35 additional information beyond the conventional vegetation reconstruction proxy of fossilised pollen:  
36 taxonomic information and spatial information. While the taxonomic benefits of phytolith analysis  
37 are reasonably well studied, the spatial scale phytolith records represent is less certain, particularly  
38 when analyses are conducted on typical palaeoecological samples taken from lake sediment.

39 There are many taxonomic benefits of phytolith analysis for palaeoecologists. For example, phytolith  
40 analysis can differentiate sub-families of Poaceae and genera of Cyperaceae, neither of which is  
41 currently possible from pollen analysis, and which can be particularly helpful in identifying different  
42 herbaceous habitats such as forest understorey, savannahs, and semi-aquatic lacustrine vegetation.  
43 Further taxonomic advantages of phytoliths include the identification of Heliconiaceae, a key  
44 disturbance indicator (Piperno, 2006), as well as other economically useful taxa unidentifiable by  
45 their pollen, such as squash (*Cucurbita*) (Bozarth, 1987) and rice (Oryzoideae) (Hilbert et al., 2017),  
46 which can provide important insights into past human land-use and human-environment  
47 interactions. Furthermore, soil surface sample work by Dickau et al. (2013) and Watling et al. (2016)  
48 have demonstrated that several neotropical ecosystems (humid evergreen forest, palm forest, semi-

49 deciduous dry forest, seasonally inundated savannah and terra firme savannah) can be  
50 differentiated based solely on the phytolith assemblage from soil samples.

51 The combination of pollen and phytolith analyses should therefore provide additional,  
52 complementary palaeoecological information. As pollen does not preserve well in soils, this can be  
53 achieved by sampling a combination of soil samples (for phytolith analysis) and lake records (for  
54 pollen analysis). However, this combination is complicated by the different spatial scales and  
55 temporal resolution provided by soil versus lake sediment records. The temporal resolution of  
56 palaeo-records from the soil column is typically significantly lower than that of lake sediment  
57 records due to bioturbation of soil via plant roots, insects and other animal disturbances which move  
58 material through the soil profile (Butler, 1995; Gabet et al., 2003). The spatial scale represented by  
59 soil samples is generally much smaller than that of lake records, as lakes act as sinks for microscopic  
60 particles from the surrounding vegetation transported via wind or water (Bennett and Willis, 2002).

61 To avoid these complications, as phytoliths preserve well in lake sediments as well as soils, both  
62 analyses can be conducted on lake sediment which would enable the same temporal resolution to  
63 be achieved for both proxies, enabling direct comparison of pollen and phytolith assemblages and  
64 providing truly complementary taxonomical and spatial information. This approach has been applied  
65 to several Late Quaternary neotropical lake records, including La Yaguada, Panama, where Late  
66 Pleistocene cooling was identified by phytoliths from montane forest taxa such as *Magnolia* and  
67 Chrysobalanaceae (Bush et al., 1992; Piperno et al., 1990) and Monte Oscuro, Panama, where a  
68 wetter Holocene climate and human disturbance were identified based on pollen and phytoliths  
69 records (Piperno and Jones, 2003). At Lagunas Granja and San José in lowland Bolivia, pollen and  
70 phytolith analyses revealed late Holocene Pre-columbian land use (Carson et al., 2015; Whitney et  
71 al., 2013). In these studies phytoliths are interpreted as representing a more local spatial scale than  
72 pollen, based on a theoretical understanding of phytolith deposition and transport, backed up in the  
73 latter two studies by comparisons with shoreline vegetation inventories.

74 Integration of pollen and phytolith records from lake sediments requires an understanding of their  
75 respective taphonomy in lakes. Piperno proposed a theoretical model of phytolith representation in  
76 lakes (Piperno, 2006, 1990) whereby phytolith source area depends largely on the lake site  
77 characteristics. For example, in stream-fed lakes in areas with high precipitation phytoliths have the  
78 potential to be transported long distances via soil erosion and runoff over land and into streams. In  
79 open, frequently burnt environments they can be transported up to 2000 km by wind. However, in  
80 closed basins surrounded by dense forest, Piperno (2006) proposes that phytoliths are likely to  
81 represent only shoreline vegetation.

82 The only published empirical study on phytolith input to lakes (Aleman et al., 2014) was conducted  
83 on three small lakes in ecosystems of central Africa: savanna, forest–savanna mosaic, and forest  
84 (0.03, 0.36, 0.14 km<sup>2</sup> respectively). Aleman found that the proportion of forest cover surrounding  
85 the lake and the number of large fires (producing ash clouds) were the main factors influencing  
86 phytolith catchment area. However, there is uncertainty over the extent to which the findings from  
87 these small lakes are representative of much larger lakes, several km in diameter, which are  
88 common throughout the tropics. In addition, these phytolith records were not compared with other  
89 vegetation proxies with an estimable source area, such as pollen, and only one sample was taken  
90 from each lake. Furthermore, the role of fire, wind and water in phytolith taphonomy in the drier,  
91 frequently burnt environments of Aleman’s study area is likely to differ from the wet environments  
92 of the Neotropics.

93 This paper therefore aims to **explore the potential value of phytoliths as a complementary proxy to**  
94 **pollen for enhancing the palaeoecological information that can be obtained from lake sediments**  
95 **in tropical lowland Bolivia.**

96 Specifically, this paper will address two questions:

- 97 I. Can humid evergreen forest, semi-deciduous dry forest and seasonally-inundated savannah  
98 ecosystems be differentiated based on phytolith assemblages from Bolivian lakes?

99 II. What are the key factors driving the composition of phytolith and pollen assemblages in  
100 these lakes, and how do they differ between proxies?

101 The approach of this study is to compare pollen and phytolith assemblages from the same lake  
102 sediment surface sample, from a suite of lakes of different sizes across different vegetation types of  
103 lowland tropical Bolivia. For some of the larger lakes, samples were analysed from multiple core sites  
104 within the lake to enable analysis of the spatial variation in phytolith assemblages across the lake  
105 compared to pollen. These assemblages were compared through ordination analyses (PCA), and  
106 potential driving factors in their differentiation were identified through constrained ordination  
107 (RDA). Comparison between these phytolith and pollen assemblages provides a useful reference  
108 point for palaeoecologists, drawing out potential areas where phytoliths from lake sediments can  
109 provide additional, useful information.

110

## 111 2. Study area and site selection

112 The study area in this paper is lowland Bolivia. This region encompasses a wide variety of vegetation  
113 types, as it is the transitional zone between the humid evergreen forests of the Amazon in the north  
114 and semi-deciduous dry forests and savannah to the south. The distribution of these ecosystems is  
115 controlled at the broad scale by climate, as precipitation decreases towards the south of the study  
116 area. At a finer scale their distribution is controlled by geology and edaphic variables, with acidic  
117 soils of Pre-Cambrian bedrock supporting *terra firme* forests, alkaline soils supporting semi-  
118 deciduous forests, and clay-rich basins supporting seasonally-inundated ecosystems (Fig. 1).

119 [Figure 1 – Map of lake sites and vegetation surveys plotted against vegetation classifications  
120 adapted from WWF terrestrial ecoregions (Olsen et al 2001) using ArcGIS 10.5.1. Lake sites are  
121 shown by red circles. Vegetation inventories and surveys are shown by black circles (IL = Vegetation  
122 survey around Lagunas Isirere and Limoncin, AC2 = Acuario 2 forest plot inventory, LF1 = Los Fierros  
123 1 forest plot inventory). Inset map of South America.]

124

125 Our study sites encompass three regions: (2.1) Chiquitania-Pantanal, (2.2) the Beni basin, and (2.3)  
126 terra firme humid evergreen forests on the Pre-Cambrian shield (Fig. 2). Lake sites were chosen from  
127 within each region to represent a range of lake sizes (Table 1).

128 [Table 1 - Summary of lake site characteristics, including references to the papers originally  
129 publishing some of the pollen and phytolith records.]

130

131 [Figure 2 - Maps of lake sites and surrounding ecosystems created using ArcGIS 10.5.1. Panel A  
132 shows the Chiquitania-Pantanal study region with Lagunas La Gaiba and Mandioré; Panel B shows  
133 terra firme humid evergreen forests on the Pre-Cambrian shield study region with Laguna Chaplin;  
134 Panel C shows the northern areas of the Beni basin study region with Lagunas Oricoré, La Luna and  
135 Granja; and Panel D shows the southern areas of the Beni basin study region with Lagunas San José  
136 and Limoncin. The locations of all surface samples are shown for each lake by black circles.  
137 Vegetation classification of the study area, based on Landsat imagery, was provided by the Museo  
138 de Historia Natural 'Noel Kempff Mercado', Santa Cruz, Bolivia, in 2015. Scale bars and latitude and  
139 longitude are presented for each individual map panel.]

140

141 **2.1. Chiquitania-Pantanal.** This region encompasses the Chiquitano semi-deciduous dry forests. Our  
142 study sites are at the eastern edge of the semi-deciduous dry forest on the Bolivia-Brazil border  
143 where it meets the Pantanal wetlands of Brazil.

144 Semi-deciduous Chiquitano dry forest is a moderately diverse transitional forest type which grades  
145 into humid evergreen forest to the north. Generally, dry forest is categorized by tree heights of 15-  
146 20 m with emergents rarely exceeding 25 m. The canopy is less closed than humid evergreen forests,  
147 allowing light to penetrate to the forest floor and develop relatively dense understory vegetation. A



148 key part of this understory is bamboo scrub, often characterised by *Guadua paniculata*. A key  
149 dominant tree species is often *Anadenanthera colubrina* of the Fabaceae family (Killeen et al., 2006;  
150 Killeen and Schulenberg, 1998) (Table 2). A detailed study of the vegetation of the eastern  
151 Chiquitano forests around Lagunas La Gaiba and Mandioré can be found in Prance and Schaller  
152 (1982).

153 [Table 2 – Vegetation inventory of Acuario 2, a 1-hectare vegetation plot just south of Noel Kempff  
154 Mercado National Park, gives a representative vegetation community composition for semi-  
155 deciduous dry forest in south-west Amazonia. Inventory conducted by recording all taxa  
156 representing >1% of the total number of stems >10 cm d.b.h. (Gosling et al., 2009).]

157 The Pantanal basin is a geographic depression surrounded by highlands which contains a floodplain  
158 that houses the world's largest tropical wetland (~135, 000 km<sup>2</sup>). The vegetation of the Pantanal is a  
159 heterogeneous mosaic of xeric, mesic and seasonally-inundated plant communities, controlled by  
160 edaphic variables, topography and flooding. Seasonally-inundated savannahs are dominant in low  
161 elevation areas, with higher elevation areas supporting inundation-tolerant gallery forests and semi-  
162 deciduous dry forests (Alho, 2005; Hamilton, 2002; Nunes da Cunha et al., 2007). Lagunas La Gaiba  
163 and Mandioré have semi-deciduous dry forest to the west and south and the Pantanal wetlands to  
164 the east and north:

165 **2.1.1. Laguna La Gaiba** is a large, shallow lake (~90 km<sup>2</sup>, depth ~4-6 m) split into two sub-basins, the  
166 deeper southern basin being largely surrounded by forest, and the shallow northern basin merging  
167 into the Pantanal wetlands (Whitney et al., 2014). Core site 6 sits to the west of the south basin, core  
168 site 10 towards the north of the south basin, and core site 16 within the northern basin (Fig. 2). Core  
169 site numbers refer to those in the original publication of pollen and diatom records from this site  
170 (Whitney et al., 2011).

171 **2.1.2. Laguna Mandioré** is a large, shallow lake (~152 km<sup>2</sup>, depth ~4 m) forming a single continuous  
172 basin. On the eastern shores dry forest grades into cerrado savannah as altitude increases (up to 846

173 m.a.s.l.) on the Amolar hill formation which separates the majority of the lake margin from the  
174 Pantanal wetlands. Core site 2 is located in the southwest of the basin and core site 5 is located in  
175 the northeast, close to the Amolar hills (Fig. 2).

176 **2.2. Beni basin.** This Amazonian sub-basin is formed by a bed of impermeable alluvial clays which  
177 permit flooding during the wet season from November to March. The geomorphology of the Beni  
178 leads to a dominance of seasonally-inundated savannah vegetation, with outcrops of humid  
179 evergreen or seasonally-dry forest on islands of Pre-Cambrian Shield within the basin (Clapperton,  
180 1993). The seasonally-inundated savannahs do not have a well-developed woody stratum but  
181 maintain a short stratum of grasses, most commonly *Paspalum lineare*, *Leptocoryoheum lanatum*,  
182 *Mesosetum sp.*, *Sacciolepis angustissima* and *Panicum parviflorum*. Islands within the wetlands are  
183 commonly formed by termite mounds which can raise an island 0.5-1.5 m above the flooded plain,  
184 allowing forest species to colonise, such as *Curatella americana* and *Davilla nitida* (Dilleniaceae),  
185 *Casearia arborea* (Salicaceae) and *Tapiria guinanensis* (Bignoniaceae) (Killeen and Schulenberg,  
186 1998) (Table 3). The lake sites from within the Beni basin are Lagunas Oricoré, La Luna, Granja,  
187 Limoncin and San José:

188 [Table 3 – Results of a qualitative vegetation survey ranking taxa as dominant, abundant, frequent or  
189 occasional in coverage from the area surrounding Lagunas Limoncin and Isirere are presented to give  
190 an example vegetation community composition for the Beni seasonally-inundated savannah. (Dickau  
191 et al., 2013).]

192 **2.2.1. Laguna Oricoré** is a large lake (~10.5 km<sup>2</sup>, depth 1-1.5 m) at the eastern edge of the Beni  
193 basin, close to the geological boundary with terra firme humid evergreen forest on Pre-Cambrian  
194 Shield bedrock. The lake is largely surrounded by seasonally-inundated savannah, with a small patch  
195 of semi-deciduous dry forest near the northeastern shore (Fig. 2). It is situated 5 km south of the  
196 evergreen forest boundary (Carson et al., 2014).

197 **2.2.2 Laguna La Luna** is a small lake (0.33 km<sup>2</sup>, depth 2 m) at the eastern edge of the Beni basin, 5  
198 km west of Laguna Oricoré. The lake is largely surrounded by seasonally-inundated savannah and  
199 adjacent to a small (7.4 km<sup>2</sup>) forest island (Fig. 2) (Carson et al., 2016).

200 **2.2.3 Laguna Granja** is a small oxbow lake (0.071 km<sup>2</sup>, depth 2 m) across the boundary from the Beni  
201 basin on the Pre-Cambrian Shield. The lake margins are dominated by riparian forest, blending into  
202 terra firme humid evergreen forest further away from the lake. To the east of the lake an area of  
203 ~0.3 km<sup>2</sup> has been cleared for cattle grazing (Fig. 2) (Carson et al., 2015).

204 **2.2.4 Laguna Limoncin** is a small lake (0.73 km<sup>2</sup>, depth 0.9 m) in the south of the Beni basin,  
205 surrounded by a mosaic of seasonally-inundated savannah and evergreen forest (Fig. 2).

206 **2.2.5 Laguna San José** is a large, shallow lake (14.3 km<sup>2</sup>, depth 1 m) in the south of the Beni basin,  
207 surrounded by a mosaic of seasonally-inundated savannah and evergreen forest. The lake is 4 km  
208 from Laguna Limoncin and has a fringing strip of riparian forest <20 m wide. The core site is located  
209 close to the northeast shoreline (Fig. 2) (Whitney et al., 2013).

210 **2.3. Terra firme humid evergreen forest.** This ecosystem is characterised by dense tall forest  
211 comprised of trees reaching 45 m in height and 1.5 m in diameter, with a closed canopy and a low  
212 density of understorey vegetation. The Moraceae family often dominates the evergreen forest  
213 canopy, while palms (Arecaceae family) are also abundant. Emergent trees can include genera from  
214 the Vochysiaceae, Fabaceae and Clusiaceae (Table 4). The rhizomatous species *Phenakospermum*  
215 *guianense* (Strelitziaceae) is locally abundant and forms huge dense colonies (Killeen and  
216 Schulenberg, 1998). The lake site from within terra firme evergreen forest is Laguna Chaplin.

217 [Table 4 – Vegetation inventory of Los Fierros 1, a 1-hectare vegetation plot within Noel Kempff  
218 Mercado National Park, gives a representative vegetation community composition for evergreen  
219 forest in south-west Amazonia. Inventory conducted by recording all taxa representing >1% of the  
220 total number of stems >10 cm d.b.h. (Gosling et al., 2005).]

221 **2.3. Laguna Chaplin** is a large, shallow, flat-bottomed lake (12.2 km<sup>2</sup>, depth 2.5 m) within the Noel  
222 Kempff Mercado National Park in eastern Bolivia, near the southern limit of Amazon humid  
223 evergreen forest. Chaplin is surrounded by humid evergreen forest with a small fringe of palm  
224 swamp and area of savannah wetland at the southwestern edge of the lake (Burbridge et al., 2004).  
225 Core site 1 is close to the centre of the lake, core site 2 is towards the east of the lake, and core site  
226 3 is close to the southern shore (Fig. 2).

## 227 3. Methods

### 228 *3.1 Use of previously published datasets*

229 This paper uses a number of previously published datasets in combination with new sample analyses  
230 (Table 1).

231 Field methods for all samples entailed long, overlapping sediment cores being retrieved using a  
232 stable floating platform and modified drop-hammer Livingston piston corer (Colinvaux et al., 1999)  
233 and shipped back to the UK in their core tubes. Surface sediments were taken using a 5-cm diameter  
234 Perspex<sup>®</sup> tube and piston to capture the uppermost unconsolidated sediments and were divided  
235 into consecutive 0.5 cm or 1.0 cm samples. These surface samples were stored in watertight plastic  
236 tubes. All samples were kept in cold storage at 4°C.

237 Standard pollen preparation protocols were followed for each of the previously published datasets,  
238 details can be found in each paper (Burbridge et al., 2004; Carson et al., 2016, 2015, 2014; Whitney  
239 et al., 2013, 2011, Plumpton et al., accepted). Chaplin 3 pollen counts are included in Figure 3 as  
240 they are the only complete pollen counts we have for Chaplin. The pollen counts for Chaplin 1 and 2  
241 have been summarised to show only the most abundant taxa, as described in Burbridge et al.,  
242 (2004). As the pollen assemblages from all three Chaplin surface samples are highly consistent with  
243 each other (Burbridge et al 2004) we use the detailed pollen assemblage from Chaplin 3 to infer  
244 likely pollen abundances at Chaplin 1 and 2 for taxa not included in the summary data e.g.  
245 Arecaceae. Phytolith extraction was conducted using the wet oxidation methods as described in

246 Piperno (2006) for each of the previously published datasets, details can be found in each paper  
247 (Carson et al., 2015; Whitney et al., 2013, Plumpton et al., accepted).

### 248 *3.2 New data analysis - laboratory methods – phytolith processing and identification*

249 New phytolith extraction and analysis was conducted on lake surface sediments from Lagunas  
250 Oricoré, La Luna, Chaplin (1 and 2) and Limoncin (Table 1). Phytolith extraction was not possible for  
251 Chaplin 3 due to lack of sample material, so phytoliths were analysed from Chaplin 1 and 2 only.  
252 Phytolith extraction was conducted using the wet oxidation method involving nitric acid heated to  
253 90°C as described in Piperno (2006). For Laguna Chaplin, 3cc of wet sediment was sampled to allow  
254 for fractionation during processing into “A” (<53 µm) and “C” (53-250 µm) fractions. For the other  
255 sites, only 1cc of wet sediment was available from the surface sample horizon, due to intensive  
256 previous study of these sites. These samples were not fractionated due to the small sediment  
257 volume available. Non-fractionated and A fraction slides were counted at 400X magnification and a  
258 minimum sum of 200 diagnostic phytoliths was counted for each sample. C fractions slides were  
259 scanned at 100X, with identifications conducted at 400X magnification. All phytoliths with taxonomic  
260 significance on the C fraction slides were counted.

261 Phytolith identification was carried out with reference to the University of Reading tropical phytolith  
262 reference collection, which contains modern specimens from 152 species, and photographs of the  
263 University of Exeter phytolith reference collection, which contains over 500 modern neotropical  
264 plant specimens. Published phytolith reference atlases were also consulted from the Neotropics,  
265 tropical Africa, Asia and Australasia (Boyd et al., 1998; Dickau et al., 2013; Iriarte and Paz, 2009;  
266 Kondo et al., 1994; Lu and Liu, 2003; Mercader et al., 2011, 2009; Piperno, 2006; D.R. Piperno and  
267 Pearsall, 1998; Dolores R. Piperno and Pearsall, 1998; Runge, 1999; Wallis, 2003; Watling et al.,  
268 2016; Watling and Iriarte, 2013). Table 5 lists all of the phytolith types identified in this study, their  
269 taxonomic association and codenames for PCA and RDA graphs.

270 [Table 5 – Phytoliths types identified with abundance >1%, their taxonomic association and PCA/RDA  
271 codes.]

### 272 *3.3 Numerical analysis*

273 For statistical analysis, phytolith samples were not analysed as separate A and C fractions despite  
274 Mandioré and Chaplin samples being fractionated during processing. In these two cases A and C  
275 fraction sums were added together as laboratory error led to large number of small phytoliths being  
276 present in the C fractions for Chaplin so samples were effectively not fractionated, and C fraction  
277 counts were so low for Mandioré (3-6 total) that they could not have been analysed separately in  
278 ordination analyses as a minimum count of 50 phytoliths is required for robust analysis (Dickau et al  
279 2013). Furthermore, summing the A and C fractions for Mandioré and Chaplin enables comparison of  
280 these records with all other lake sites studied which had insufficient sediment available for  
281 fractionation.

282 Frequency plots for phytoliths and pollen taxa were created using version 1.7 of the C2 software  
283 (Juggins, 2016). Ordination analyses were conducted and plotted using the vegan 2.5-2 package  
284 (Oksanen et al., 2018) in R 3.4.1. Only taxa with >1% abundance were included in the analysis.

285 Abundances were square-root transformed (the Hellinger transformation) prior to analysis.

286 Detrended correspondence analysis (DCA) of summed counts demonstrated relatively short  
287 environmental gradients in the dataset, therefore Principal Component Analysis (PCA) was chosen  
288 for ordination of the phytolith and pollen assemblages, and Redundancy Analysis (RDA) for  
289 constrained ordination. The environmentally constraining variables considered were: lake size,  
290 distance of core site to shore, and average tree cover from local to regional scale (within 100, 1000,  
291 5000, 10000 and 20000 m radius from the lake shore). Permutation tests were conducted on the  
292 RDA model to assess the statistical significance of the environmental constraining variables as  
293 predictors of the variation in pollen and phytolith assemblages (Borcard et al., 2011; ter Braak and  
294 Verdonschot, 1995). For both the pollen RDA and phytolith RDA, an ANOVA “by term” (i.e.

295 environmental variable) was conducted with 999 permutations in R 3.4.1 using vegan 2.5-2 (Oksanen  
296 et al., 2018).

### 297 *3.3.1 Spatial analyses - GIS*

298 Tree cover data within 100, 1000, 5000, 10000 and 20000m radius from the lake shore were  
299 extracted from the Hansen et al. (2013) dataset using the following method. The circumference of  
300 each lake site was traced using Google Earth Pro geometry tools and these layer files were converted  
301 to shape files using QGIS 2.14.0. Buffer zones around each lake site were created using the buffer  
302 tool in ArcGIS 10.4 at distances of 100, 1000, 5000, 10000 and 20000m from the lake shorelines.  
303 Tree cover data was then extracted from within each buffer zone and mean tree cover calculated  
304 using packages rgdal 1.4-4 (Bivand et al., 2019), raster 2.9-5 (Hijmans, 2019), and maptools 0.9-5  
305 (Bivand and Lewin-Koh, 2019) in R 3.4.1. Lake area and distance of core site to shore were calculated  
306 using Google Earth Pro geometry tools.

## 307 *4. Results*

### 308 *4.1 Key trends in phytolith and pollen assemblages from each region*

#### 309 *4.1.1 Chiquitania-Pantanal semi-deciduous dry forest – Lagunas Mandioré and La Gaiba*

310 [Figure 3 – Summary diagram of phytolith abundances from all lakes studied, presented as  
311 percentage data. Vegetation surrounding the lakes has been classified into 3 ecosystem types: semi-  
312 deciduous dry forest (Chiquitania-Pantanal), seasonally inundated forest-savannah (Beni basin), and  
313 evergreen forest (PCS Humid Evergreen Forest).]

314

315 [Figure 4 – Summary diagram of pollen abundance from all lakes studied, presented as percentage of  
316 terrestrial total. Vegetation surrounding the lakes has been classified into 3 ecosystem types: semi-  
317 deciduous dry forest (Chiquitania-Pantanal), seasonally inundated forest-savannah (Beni basin), and  
318 evergreen forest (PCS Humid Evergreen Forest). Pollen data for Chaplin 1 and 2 is only available in

319 highly summarised format with data for a restricted number of taxa. Full pollen counts are available  
320 for Chaplin 3.]

321

322 The two surface samples from Laguna Mandioré (Fig. 2) show consistent phytolith assemblages with  
323 high Poaceae phytolith total abundances (67-71%), with significant contributions from Bambusoid  
324 (19-24%) and Panicoid types (22-29%) (Fig. 3). Arboreal phytoliths make up 22-26% of the  
325 assemblage (Fig. 3). The three surface samples from Laguna La Gaiba (Fig. 2) show lower Poaceae  
326 phytolith total abundances (50-62%), largely due to lower abundances of Panicoid types (6-13%)  
327 than the Laguna Mandioré samples (Fig. 3). Arboreal phytoliths comprise 18-35% of the assemblages  
328 at Laguna La Gaiba, showing greater variation than the Laguna Mandioré samples. This is driven by  
329 the higher arboreal phytolith abundance at La Gaiba 6 compared to La Gaiba 10 and 16, which are  
330 more consistent with each other (Fig. 3).

331 Overall, both lake sites in the Chiquitania-Pantanal semi-deciduous dry forest have a high percentage  
332 of Poaceae phytoliths (50-71% of total assemblage). A large proportion of this Poaceae total is  
333 Bambusoid phytoliths at 17-24%. Cyperaceae phytolith abundance in the semi-deciduous forest  
334 samples is the highest of the three ecosystem types studied ranging from 5-9% of total. Arboreal  
335 phytolith totals are largely comprised of non-Arecaceae types. The most abundant arboreal taxa in  
336 semi-deciduous dry forests, such as Fabaceae (including *Anadenanthera*) and Bignoniaceae  
337 (including *Tabebuia*) (Table 2), cannot be differentiated to family or genus level using phytoliths  
338 (Piperno, 2006). However, these taxa would contribute to the phytolith arboreal indicators such as  
339 globular granulates and faceted elongates within the woody eudicot category (Fig. 3).

340 Pollen assemblages from the Chiquitania-Pantanal samples are reasonably consistent, showing the  
341 highest *Anadenanthera* (4%) and *Astronium* (3%) and lowest Moraceae/Urticaceae (0%) pollen  
342 abundances of all samples studied (Fig. 4). The total arboreal pollen abundance is constant across  
343 the samples at 18-29%, except La Gaiba 16 at 6%. This pattern broadly fits with the total arboreal



344 phytolith abundances where La Gaiba 16 is also low at 18%, but so are La Gaiba 10 and Mandioré 5  
345 at 21% and 22% respectively (Fig. 3). The samples from Lagunas Mandioré and La Gaiba also show  
346 the highest Poaceae pollen abundance of all samples studied at 42-56% (Fig. 4). These pollen results  
347 are in contrast to the Poaceae phytolith abundances, which are similar between semi-deciduous dry  
348 forest sites and Beni seasonally-inundated forest-savannah mosaic sites (Fig. 3). There is also  
349 stronger variation in Cyperaceae pollen abundance, ranging from 7% to 34%, than Cyperaceae  
350 phytolith abundances which range from 5% to 9%.

#### 351 4.1.2 Beni seasonally-inundated savannah-forest mosaic – Lagunas Oricoré, La Luna, Granja, Limoncin 352 and San José.

353 Phytolith assemblages from the Beni basin lakes within seasonally-inundated savannah-forest  
354 mosaic have consistently high grass and herb phytolith totals, between 75% and 85% of total  
355 assemblage (Fig. 3). For most lake sites this total is dominated by Poaceae phytoliths, except Laguna  
356 San José which has a significant contribution of herbs such as Heliconiaceae, Marantaceae and  
357 Asteraceae (11%, 15% and 12% of total assemblage respectively). All other samples from the Beni  
358 lakes contain low (<6%) abundances of phytoliths from these herbs, or they are absent (Fig. 3).  
359 Across all samples from Beni lakes, the composition of the Poaceae phytolith total varies with  
360 particularly high Panicoid phytolith abundance at Laguna Granja (51%), and high Bambusoid  
361 phytolith abundance at Lagunas La Luna and Limoncin (23% and 20% respectively). Cyperaceae  
362 phytoliths appear at low abundance in all samples from the Beni, except Laguna San José where they  
363 are absent (Fig. 3). Total arboreal phytolith abundance is the lowest of all ecosystems studied,  
364 ranging from 12% at Laguna Limoncin to 26% at Laguna Granja. Arecaceae phytoliths make up a  
365 significant proportion of arboreal types at Lagunas Limoncin and San José, whereas woody eudicot  
366 phytolith types dominate at Lagunas Oricoré, La Luna and Granja (Fig. 3).

367 Pollen assemblages from the Beni basin lakes show significant variation in total arboreal pollen  
368 abundance, driven largely by the low abundance of Moraceae/Urticaceae pollen at Laguna Limoncin

369 (2%) and Laguna San José (5%), compared to 19% at Laguna Oricoré (Fig. 4). This pattern matches  
370 that in the phytolith assemblages, where Laguna Limoncin has the lowest total arboreal phytolith  
371 abundance at 12% (Fig. 3). The abundance of Arecaceae phytoliths at Lagunas Limoncin and San José  
372 of 9% and 16% respectively, is not reflected in the pollen assemblage where Arecaceae pollen is  
373 absent for both sites (Fig. 4). *Cecropia* pollen abundance is highest at Lagunas San José and Granja at  
374 15% and 13% respectively (Fig. 4). There is significant variation in Cyperaceae pollen abundance with  
375 particularly low levels at Oricoré and La Luna (10% and 6% respectively) compared to Limoncin and  
376 Granja (39% and 31% respectively). Overall, the samples show more variation in total grass and herb  
377 pollen than total grass and herb phytoliths, with Limoncin and Granja showing significantly higher  
378 grass and herb pollen totals than the other samples (Fig. 4).

#### 379 4.1.3 Terra firme humid evergreen forest – Laguna Chaplin

380 The two phytolith samples from Laguna Chaplin within terra firme evergreen forest are  
381 differentiated from the samples from other ecosystems by the high abundance of Arecaceae  
382 phytoliths (53-59% of total assemblage) (Fig. 3). Other arboreal phytolith types are present in similar  
383 abundance to semi-deciduous forest assemblages, ranging from 16-22%. Grass and herb phytolith  
384 abundances are the lowest of all samples studied at 19-30% of the assemblage, with low abundances  
385 of all Poaceae (13-25%) and Cyperaceae (2%) phytolith types but particularly low abundances of  
386 Bambusoid types (5-6%). The surface sample closer to the shore (Chaplin 2) shows a higher  
387 abundance of Poaceae and lower arboreal phytoliths than the more central surface sample (Chaplin  
388 1).

389 The complete pollen assemblage from Laguna Chaplin (Chaplin 3) shows the lowest Poaceae (4%)  
390 and highest total arboreal pollen (76%) abundance of all samples studied (Fig. 4), matching the  
391 pattern shown in the phytolith assemblages from Laguna Chaplin (Chaplin 1 and 2) (Fig. 3). Within  
392 this total arboreal figure, pollen abundance is made up largely of Moraceae/Urticaceae (48%) with

393 some *Cecropia* (9%) and *Alchornea* (5%) pollen. This assemblage is in contrast to the phytoliths,  
394 where arboreal phytolith types are dominated by Arecaceae phytoliths (53-59%).

#### 395 4.2 PCA results

396 [Figure 5 – PCA biplot for a) phytolith and b) pollen data. Axes are Principal Component 1 (PCA1) and  
397 Principal Component 2 (PCA2). The percentage in parentheses on these axes is the percentage of  
398 variance in the dataset explained by that principal component. Lake sites are coloured according to  
399 the ecosystem they represent: light green = semi-deciduous dry forest, yellow = Beni seasonally-  
400 inundated forest-savannah mosaic, dark green = humid evergreen forest. Taxa are presented in  
401 black. Codes for taxa names are presented in Tables 5 and 6 for phytoliths and pollen respectively.]

402

403 PCA of the phytolith dataset (Fig. 5) shows differentiation of the terra firme evergreen forest  
404 samples (Chaplin 1 and 2) from all other samples studied in this paper, largely by PCA1. PCA1  
405 explains 42% of the variance in the dataset and is driven largely by the abundance of Arecaceae  
406 phytolith types (labelled Palm in Fig. 5, see Table 5 for full list of phytolith PCA codenames). PCA1 is  
407 positively correlated with abundance of Arecaceae, Heliconiaceae and Marantaceae types and  
408 negatively correlated with Poaceae types, such as Panicoid crosses, rondels and bulliforms (Fig. 5).  
409 All other samples plot negatively on PCA1, except Laguna San José. PCA2 explains 20.5% of the  
410 variance in the dataset and is correlated positively with Panicoid crosses and negatively with  
411 Poaceae and Bambusoid bulliform phytolith types (Fig. 5). This axis separates sites with higher  
412 Panicoid abundances, such as Laguna Granja which is at present surrounded by agricultural land and  
413 Laguna Mandioré which is close to upland savannah, from sites with less Panicoid inputs such as  
414 Laguna La Gaiba.

415 PCA of the pollen dataset (Fig. 5) shows clear differentiation of the terra firme evergreen forest  
416 sample (Chaplin 3) from all other samples by PCA1, which is positively correlated with abundance of  
417 Moraceae/Urticaceae pollen and also *Celtis* and *Isoetes* (see Table 6 for a list of pollen PCA

418 codenames). The two samples from Laguna Mandioré, within Chiquitania-Pantanal, are also clearly  
419 differentiated from all other samples as they plot negatively on PCA1, correlated with abundance of  
420 Poaceae, *Anadenanthera* and *Eichhornia*. Both Chaplin and Mandioré samples plot positively on  
421 PCA2, correlated with low abundance of Cyperaceae, *Typha* and *Cecropia* pollen. The samples from  
422 Laguna La Gaiba, within Chiquitania-Pantanal, plot negatively on PCA1 and PCA2, as do samples from  
423 the Beni basin samples from Lagunas Limoncin, San José and Granja. Samples from Lagunas Oricoré  
424 and La Luna are differentiated by plotting slightly positively on PCA1 and PCA2 (Fig. 5).

425 [Table 6 – Pollen taxa identified with abundance >1% and PCA/RDA codes.]

426 Laguna La Gaiba has three surface samples (6, 10, 16), Laguna Mandioré has two (2, 5) and Laguna  
427 Chaplin has three (1, 2, 3). The phytolith PCA results generally show clustering by lake, with the two  
428 Chaplin samples and the three La Gaiba samples plotting together (Fig. 5). Chaplin samples 1 and 2  
429 are particularly closely grouped. For La Gaiba, samples 6, 10 and 16 are also closely clustered, but  
430 with some overlap with lake sites from the Beni i.e. Oricoré. Mandioré samples 2 and 5 cluster  
431 within the same quadrant of the phytolith PCA but are not closely grouped (Fig. 5). In comparison,  
432 the pollen PCA results show tighter clustering of the Mandioré samples than the La Gaiba samples,  
433 although both are clearly grouped (Fig. 5).

#### 434 *4.3 RDA results*

435 [Figure 6 – RDA tri-plot for a) phytolith and b) pollen data. Axes are Redundancy Analysis 1 (RDA1)  
436 and 2 (RDA2). The percentage in parentheses on these axes is the percentage of variance in the  
437 dataset explained by that component. Environmental constraining variables are presented in blue:  
438 lake area, distance of core site to lake shore, and tree cover within 100, 1000, 2000, 10,000 and  
439 20,000 m of the lake shore. Lake sites are coloured according to the ecosystem they represent: light  
440 green = semi-deciduous dry forest, yellow = Beni seasonally-inundated forest-savannah mosaic, dark  
441 green = humid evergreen forest. Taxa are presented in black. Codes for taxa names are presented in  
442 Tables 5 and 6 for phytoliths and pollen respectively.]

443

444 The pollen RDA (Fig. 6) shows that lake area and distance of core site to shore are both strongly  
445 negatively correlated with axes 1 and 2, explaining the differentiation of large lakes such as  
446 Mandioré from smaller lakes such as Granja. Tree cover at 1,000 – 20,000 m is also negatively  
447 correlated with axes 1 and 2, although more strongly with axis 2, particularly for tree cover at 20,000  
448 m. Axis 2 represents the differentiation of highly forested sites such as Chaplin and Mandioré, from  
449 sites in more open savannah-lake landscapes such as Limoncin, Granja, San Jose and to a lesser  
450 extent La Gaiba. The results of the permutation test show that lake area, tree cover at 100 m and  
451 tree cover at 20,000 m are the most statistically significant environmentally constraining variables  
452 ( $p=0.001$  for all three variables) (S1). Tree cover at 10,000 m and 5,000 m are also statistically  
453 significant explanatory variables ( $p=0.008$  and  $p=0.023$  respectively) (S1).

454 The phytolith RDA (Fig. 6) shows that while tree cover at 1,000 - 20,000 m is positively correlated  
455 with axis 1, the strongest correlation with axes 1 and 2 is tree cover at 100 m. Lake area and distance  
456 to shore are both negatively correlated with axis 1. The results of the permutation test show that the  
457 most statistically significant environmentally constraining variable is tree cover at 100 m ( $p=0.001$ ),  
458 followed by tree cover at 5,000 m ( $p=0.002$ ) (S2).

## 459 5. Discussion

### 460 5.1 Differentiating ecosystems

461 Based on the phytolith assemblages of lake records studied here it is possible to differentiate humid  
462 evergreen forest from semi-deciduous forest and Beni seasonally-inundated savannah-forest mosaic  
463 sites, largely by the high abundance of *Arecaceae* phytoliths, but not possible to differentiate semi-  
464 deciduous forest from seasonally inundated savannah-forest mosaics (Fig. 5). This contrasts with the  
465 findings of Dickau et al. (2013) who were able to differentiate these ecosystems, based on soil  
466 samples from within Noel Kempff Mercado National Park (NKMNP) and the shorelines of Lagunas  
467 Limoncin and Isirere in the Beni Basin. There are two main differences between the phytolith

468 assemblages from lakes in this study and those in soil samples from the same ecosystems, as  
469 described by Dickau et al. (2013). Firstly, in semi-deciduous forest sites our lake records contain less  
470 Bambusoid phytoliths than Dickau's soil samples, with less consistent *Olyrae* and *Chusquea*  
471 phytoliths. Secondly, in seasonally-inundated savannah-forest mosaic sites the lake samples contain  
472 less (or less consistent) Heliconiaceae, Asteraceae, and Marantaceae phytoliths than Dickau's soil  
473 samples.

474 There are several possible reasons for the differences between the assemblages from the lakes  
475 studied here and the soil samples studied by Dickau. Firstly, the soil samples studied in Dickau et al.  
476 (2013) are from 1-hectare plots within closed canopy and continuous forest or savannah  
477 ecosystems, while the lake samples studied here are surrounded by heterogeneous landscapes. For  
478 example, the dry forest signal at Lagunas La Gaiba and Mandioré may be diluted by neighbouring  
479 ecosystems in the catchment such as the seasonally-inundated savannahs of the Pantanal wetlands  
480 or the upland savannah of the Amolar hills (Fig. 2). Furthermore, the lake sites from the Beni basin  
481 are spread across a large area (Fig. 1). Vegetation survey data from Lagunas Limoncin and Isirere  
482 (Table 3) in the south of the Beni basin shows dominance of Marantaceae (*Thalia genticulata*) and  
483 abundance of Heliconiaceae (*Heliconia sp.*), but similar surveys from Lagunas La Luna and Granja in  
484 the north of the Beni basin show Heliconiaceae is not present at all and Marantaceae only at Laguna  
485 La Luna (Carson et al., 2016, 2015). Therefore, key phytolith types that enabled the differentiation of  
486 Beni samples by Dickau et al., (2013) are not present across all Beni sites. The heterogeneity of the  
487 vegetation of the Beni basin may prevent these phytolith types from being used as indicators of Beni  
488 phytolith assemblages. Additional lake sites need to be studied from within these ecosystems before  
489 these findings can be generalised.

490 Secondly, the lack of fractionation of phytolith samples in this study may have contributed to the  
491 differences in assemblages as large-sized phytoliths such as Asteraceae platelets, Marantaceae seed  
492 and nodular phytoliths, and hairbases, tracheids and sclerids from woody eudicots would not have

493 been concentrated into the C-Fraction. Previous studies have found that the C-Fraction  
494 differentiates neotropical ecosystems more easily than the A-Fraction (Dickau et al., 2013; Watling  
495 et al., 2016). However, due to the small size of lake sediment samples, it is often not possible to  
496 fractionate during phytolith processing. This is a key consideration for planning of future studies of  
497 phytoliths from lake sediment. To ensure sufficient sediment is available, it may be necessary to  
498 collect several replicate lake cores.

499 In comparison, the pollen assemblages from the lakes studied here differentiated all three  
500 ecosystems (humid evergreen forest, seasonally inundated savannah-forest mosaic and semi-  
501 deciduous dry forest) (Fig. 4, 5). This finding corroborates pollen trap studies of 1-ha plots where  
502 these three ecosystems were differentiated by their modern pollen assemblages (Gosling et al.,  
503 2009, 2005; Jones et al., 2011). Fossil pollen assemblages from lakes have also revealed changes  
504 between these ecosystems across south-west Amazonia (e.g. Whitney, Mayle, et al. 2013; Carson et  
505 al. 2015; Carson et al. 2016). Pollen can be used to differentiate a larger number of arboreal taxa  
506 than phytoliths, such as *Anadenanthera* and *Astronium* pollen, which is indicative of dry forest  
507 (Gosling et al., 2009), thus enabling differentiation of different forest types. However, for  
508 understorey and herbaceous vegetation, the pollen record is significantly weaker, particularly for  
509 Poaceae sub-families which are challenging to differentiate using pollen alone (Julier et al., 2016).  
510 Herbaceous taxa can be more effectively differentiated by their phytoliths than by their pollen; e.g.  
511 Poaceae sub-families such as bamboos and oryzoid (rice) types (Piperno, 2006). Identification of  
512 these taxa from the phytolith record can assist with ecosystem differentiation as well as provide  
513 important archaeological information on human activities (Hilbert et al., 2017; Watling et al., 2018,  
514 2017). Whilst in these lakes phytolith analysis alone was not be able to differentiate all three  
515 ecosystems, it has added taxonomic value; e.g., the differentiation between understorey grass taxa  
516 such as bamboos within semi-deciduous dry forest versus savannah grasses from the Panicoideae  
517 sub-family. This distinction allows identification of changes in upland savannah compared to changes

518 in forest understorey at lake sites like Laguna Mandioré, which would not be possible from the  
519 Poaceae pollen record alone.

## 520 *5.2 Key factors driving the composition of phytolith and pollen assemblages in lakes*

521 Some of the variation between our lake samples is driven by the surrounding ecosystem, but as the  
522 PCA results show (Fig. 5), this does not account for all of the variation between samples. Other  
523 factors are influencing the phytolith and pollen assemblages beyond the surrounding ecosystem. In  
524 order to usefully interpret the fossil phytolith assemblages from these lakes, it is necessary to  
525 understand these influences. Pollen assemblages are used as a reference point for comparison with  
526 the phytolith assemblages, and to highlight the relative strengths of each proxy for palaeo-vegetation  
527 reconstructions. This analysis has highlighted three key factors driving the composition of phytolith  
528 assemblages in lakes: productivity, taphonomy, and lake size.

### 529 5.2.1 Productivity

530 As with pollen, different taxa produce different quantities of phytoliths (Piperno, 2006, 1985).  
531 Arecaceae are high phytolith producers (Piperno, 2006) and are therefore overrepresented in the  
532 phytolith record (Aleman et al., 2014; Bremond et al., 2005). The phytolith assemblages from Laguna  
533 Chaplin within evergreen forest show Arecaceae phytolith abundance to be 53-59%, in contrast to  
534 the vegetation inventory from a 1-ha plot in evergreen forest in Noel Kempff Mercado National Park,  
535 TF-1 (Table 4), which shows that Arecaceae accounts for only ~9% of stems. This finding  
536 corroborates Dickau et al (2013) who also found over-representation of Arecaceae phytolith types in  
537 the soils sampled from terra firme evergreen forest, but at 30% of the assemblage. In a study of  
538 surface soil samples in Acre state Brazil, Watling et al. (2016) found similar Arecaceae phytolith  
539 abundances in evergreen forest, but 65% in palm forest. This finding puts the Arecaceae phytolith  
540 abundances found at Chaplin more closely in-line with those from palm forest than humid evergreen  
541 forest. However, additional lakes from evergreen forest would need to be sampled to clarify  
542 whether the super-abundance of Arecaceae phytoliths is a consistent pattern across humid



543 evergreen forest lake records, or a particular feature of Laguna Chaplin due to the narrow palm  
544 swamp fringe at the southern shoreline.

545 In stark contrast to the phytolith record, the modern pollen assemblage from Laguna Chaplin has  
546 very low Arecaceae abundance (<3%). Therefore, Arecaceae is markedly over-represented in the  
547 phytolith record (53-59%) relative to the TF-1 plot vegetation inventory from humid evergreen forest  
548 in NKMNP, north-eastern Bolivia (9%), but is markedly underrepresented in the pollen record (<3%).  
549 These relationships clearly have an important bearing on the interpretation of Arecaceae pollen and  
550 phytolith fossil records from evergreen forest, especially in the context of the on-going debate over  
551 whether high abundance of Arecaceae signifies pre-Columbian forest management (Rull and  
552 Montoya, 2014; Watling et al., 2017).

### 553 5.2.2 Taphonomy

554 It is likely that different taphonomic processes are driving the deposition of phytoliths in soil and  
555 lake sediment settings. While the phytolith assemblage in soil is likely to be dominated by phytoliths  
556 deposited directly from plants *in situ*, phytoliths in lake sediments will have been transported from  
557 the surrounding vegetation. The theoretical model of phytolith transport into lakes proposed by  
558 Piperno (2006) suggests that in dry, open environments with frequent burning they will be  
559 transported by wind (Aleman et al., 2014), but in wet, closed environments they will be transported  
560 by water run-off over land or via stream and river inputs to the lake. This theory therefore suggests  
561 that in dry, open environments with frequent burning phytoliths may be transported long distances  
562 by wind, similarly to pollen, and therefore represent large catchment areas. However, in wet  
563 environments with closed-canopy forest vegetation, where transport is primarily via water,  
564 phytoliths would be likely to represent more local vegetation, depending on precipitation and  
565 flooding regimes. Closed-basin lakes fed largely by water run-off over land would be likely to present  
566 highly local records, whereas lakes with stream and river inputs could collect phytoliths transported  
567 from greater distances.

568 The lakes studied here are from humid environments of Amazonian Bolivia, where precipitation  
569 ranges from 1000 - 2000 mm/year (Seiler et al., 2013) with forest vegetation in continuous or mosaic  
570 distributions (Killeen et al., 2006; Killeen and Schulenberg, 1998; Whitney et al., 2013). The RDA  
571 results demonstrate that local (100 m) tree cover is a stronger driver of variation in phytolith  
572 assemblages between these lakes than extra-local (1,000 m) and regional (20,000 m) tree cover (Fig.  
573 6). These results suggest that phytolith records from these lakes are predominantly representing  
574 vegetation at the local scale (100 m from the lake shore), with only limited inputs from extra-  
575 local/regional sources (1,000 – 20,000 m of the lake shore). This finding supports Piperno's theory  
576 that in wet environments phytoliths are transported by water, primarily over-land. Even in the  
577 seasonally flooded landscape of the Beni basin and in lakes receiving an annual flood pulse from the  
578 Paraguay river (McGlue et al., 2012), our results suggest the primary method of phytolith transport  
579 into the lakes is likely to be local water run-off over land with the phytolith records largely  
580 representing local vegetation within 100 m of the shore. Tree cover at 1,000 – 20,000 m was found  
581 to be a weaker driver of variation in the phytolith assemblages than tree cover at 100 m, but  
582 nevertheless still exerted an influence (Fig. 6). The influence of this 'extra-local' vegetation may be  
583 due to the seasonal flooding regimes in the flat Beni and Chiquitano-Pantanal landscapes, whereby  
584 phytoliths may be transported longer distances by flood waters.

585 This transport via water is likely to have a bias towards smaller, lighter phytoliths over long  
586 distances, potentially reducing the number of large C Fraction sized phytoliths in lake records. This  
587 bias is also true for pollen transport within lakes, whereby larger pollen grains, such as maize, are  
588 preferentially deposited closer to the lake shore. This potential size bias in taphonomy may lead to  
589 fewer large C Fraction phytoliths in lake sediments, e.g. Asteraceae and Marantaceae which can be  
590 important for differentiating ecosystems (Dickau et al., 2013; Watling et al., 2016). Larger lake-  
591 sediment samples may therefore be necessary for recovering sufficient C Fraction phytoliths.

592 This study has provided empirical evidence to support the hypothesis that pollen assemblages in  
593 lake samples represent a larger catchment area than that of phytolith assemblages. This is  
594 demonstrated by the pollen RDA results which show that the key environmental variables driving  
595 the differences between pollen assemblages across lake sites in our study region are lake area and  
596 tree cover at 20,000 m (Fig. 6). This suggests that pollen records most strongly represent vegetation  
597 at a regional scale (20,000 m from lake shore). This is in alignment with studies of pollen taphonomy  
598 and catchment area (Bunting et al., 2004; Sugita, 1994), which demonstrate that while other factors  
599 such as pollen productivity, grain fall speed, atmospheric turbulence and wind speed have an  
600 influence, pollen records from large lakes generally represent larger catchment areas. This is  
601 supported by the co-correlation of lake area and tree cover at 1,000 - 20,000 m in the pollen RDA  
602 plot (Fig. 6). Pollen records are therefore most strongly influenced by regional vegetation (20,000 m)  
603 scales, while phytolith records are most strongly influenced by local (100 m) vegetation.

604

### 605 5.2.3 Lake Size

606 The lakes studied here encompass a wide range of sizes, from Laguna Granja at 0.071 km<sup>2</sup> to Laguna  
607 Mandioré at 152 km<sup>2</sup> in area. The RDA results (Fig. 6) demonstrate that lake size does influence  
608 phytolith assemblage composition, although it is not statistically significant at the 95 % confidence  
609 level ( $p=0.059$ ). By contrast, lake size has a statistically significant influence on the pollen  
610 assemblage ( $p=0.001$ ). The strong influence of local (100 m) vegetation on the phytolith assemblage  
611 would suggest that, in larger lakes in particular, the assemblage will be strongly influenced by the  
612 vegetation type near to the sample site. This can be seen in the within-lake variation in phytolith  
613 assemblages from the large lakes Lagunas Mandioré, La Gaiba and Chaplin, reflecting differences in  
614 local vegetation around the lake.

615 For example, Mandioré sample 5 is located in the north-east of the lake basin, close to the Amolar  
616 upland savannah which contains a high proportion of Panicoid taxa. The phytolith record reflects this

617 with a higher Panicoid abundance and lower Bambusoid and arboreal abundance. Mandioré 2 is  
618 located in the south-west of the basin surrounded by seasonally dry tropical forest, which is  
619 reflected in the higher Bambusoid and arboreal phytolith abundance at this core site. At La Gaiba,  
620 the differences in assemblage between core sites are related to the proximity to the Pantanal  
621 wetlands. La Gaiba 6 is in the centre of the south basin, where the surrounding lake shores are  
622 dominated by semi-deciduous forest. This sample position is reflected in the higher arboreal  
623 phytolith abundances and lower grass and herb abundances. Towards the north end of the south  
624 basin (La Gaiba 10) and into the north basin (La Gaiba 16), the semi-deciduous forest merges into the  
625 Pantanal wetlands. These wetlands likely contribute to the higher grass and herb phytolith totals  
626 found in these two samples. At Chaplin, the core site closer to the shore (Chaplin 2) shows a higher  
627 abundance of Poaceae and lower arboreal phytoliths than the more central site (Chaplin 1), possibly  
628 reflecting greater inputs from local vegetation, including an area of savannah marsh at the south  
629 west shoreline.

630 For these three large lakes, the level of within-lake spatial variation is greater in the phytolith  
631 assemblages than the pollen assemblages, as shown by the groupings in the PCA results (Fig. 5).  
632 While some differentiation in the pollen assemblage can be seen at La Gaiba depending on proximity  
633 to the Pantanal wetlands, it is not as strong as the variation in the phytolith assemblage (Fig. 4, 5).  
634 This supports the finding that phytolith assemblages are more heavily influenced by local vegetation  
635 than pollen assemblages. The different spatial scales that these two vegetation proxies represent  
636 provide a valuable opportunity for enhancing the ecological detail that can be extracted from  
637 palaeoecological records. Not only do the two proxies provide complementary taxonomic  
638 information, but they also provide vegetation information at complementary spatial resolution. A  
639 sediment core from a large lake can therefore be used to reconstruct regional vegetation using the  
640 pollen record, and local vegetation using the phytolith record.

641

## 642 6. Conclusions

643 Phytolith analysis of lake sediments, particularly when integrated with pollen analysis, has  
644 demonstrated potential for enhancing the ecological detail in Neotropical palaeo-vegetation  
645 reconstructions.

646 1. It is possible to differentiate evergreen forest from semi-deciduous forest and Beni seasonally  
647 inundated savannah- forest mosaic using the phytolith assemblage from lake samples alone, largely  
648 based on the abundance of *Arecaceae* phytolith types. It was not possible in this study to  
649 differentiate semi-deciduous forest from seasonally inundated savannah- evergreen forest mosaics  
650 from the Beni Basin using phytoliths alone.

651 2. Empirical analysis demonstrated that in the ecosystems studied here, phytolith assemblages in  
652 lake sediment records are most strongly influenced by local (within 100 m of the lake shore)  
653 vegetation and therefore likely to be transported via water run-off over land rather than long-  
654 distance travel via wind. This leads to significant spatial variation in phytolith assemblages within  
655 large lakes which have a diversity of vegetation types in their local catchment. Pollen and phytoliths  
656 from lake sediment samples from large lakes therefore represent different spatial scales: pollen  
657 represents extra-local or regional vegetation; phytoliths represent local or shoreline vegetation.

658 3. Phytoliths from lake sediment core samples can reveal the history of local vegetation. Therefore,  
659 sediment cores from large lakes can be used to assess the regional vegetation using pollen, and the  
660 local vegetation using phytoliths. However, while a pollen record from a single lake core is sufficient  
661 to record the regional vegetation, multiple cores across large lakes are likely to be needed for  
662 phytolith analysis to adequately capture spatial variation in local/shore-line vegetation around the  
663 lake.

### 664 6.1 Future work

665 To build our understanding of the spatial scale phytoliths from lakes represent under different  
666 environmental conditions, further studies on phytolith taphonomy are needed. Mechanistic and

667 experimental studies of phytolith taphonomy would provide a solid basis for interpretation of  
668 observations from field studies. Additionally, this study was limited to only three ecosystems, not  
669 including upland terra firme savannah. The influence of long-distance dispersal by wind in open  
670 savannah-dominated, drier environments may have a significant impact on the spatial scale the  
671 phytolith records represent (Aleman et al., 2014). Also, the specific characteristics of the lake sites  
672 chosen for this study will have affected the results. For example, the proximity of the Pantanal  
673 wetlands to both semi-deciduous dry forest lake sites is likely to have influenced the results.  
674 Furthermore, as only one lake - Chaplin - from within humid evergreen forest was studied, it is  
675 difficult to generalise to all lake records within this ecosystem. For example, if a study area of humid  
676 evergreen forest does not contain palms, it may not be possible to differentiate it from other forest  
677 types using phytoliths alone. Therefore, further studies including additional ecosystems and greater  
678 numbers of lakes is needed to confirm these findings.

679

## 680 [Acknowledgements](#)

681 We thank all of our colleagues who contributed lake sediment material for phytolith analysis and/or  
682 pollen or phytolith data from lake surface samples: John Carson, Jennifer Watling, and Ruth Dickau.  
683 Funding to collect these sediment samples was provided by: The Leverhulme Trust, National  
684 Geographic, The Royal Society, NERC. We acknowledge the Royal Botanic Gardens Edinburgh (RBGE),  
685 Museo Natural Historia Noel Kempff Mercado (MNHNKM) and Jose Iriarte of the University of Exeter  
686 for herbarium material used for phytolith identification. We also thank Jose Iriarte for his support  
687 and training in phytolith processing techniques and identification. Laboratory and numerical  
688 analyses and writing of the paper were funded through H.P.'s PhD funding from the University of  
689 Reading, UK. We would also like to thank the editor and two anonymous reviewers for their  
690 comments and suggestions, which helped greatly improve this manuscript.

691 Declarations of interest: none.

692   References

- 693   Aleman, J.C., Canal-Subitani, S., Favier, C., Bremond, L., 2014. Influence of the local environment on  
694       lacustrine sedimentary phytolith records. *Palaeogeogr. Palaeoclimatol. Palaeoecol.* 414, 273–  
695       283. <https://doi.org/10.1016/j.palaeo.2014.08.030>
- 696   Alho, C.J.R., 2005. The Pantanal, in: Fraser, L.H., Keddy, P.A. (Eds.), *The World’s Largest Wetlands:  
697       Ecology and Conservation*. Cambridge University Press, Cambridge, pp. 203–271.
- 698   Bennett, K.D., Willis, K.J., 2002. Pollen, in: *Tracking Environmental Change Using Lake Sediments*.  
699       Kluwer Academic Publishers, Dordrecht, pp. 5–32. [https://doi.org/10.1007/0-306-47668-1\\_2](https://doi.org/10.1007/0-306-47668-1_2)
- 700   Bivand, R., Keitt, T., Rowlingson, B., 2019. rgdal: Bindings for the “Geospatial” Data Abstraction  
701       Library. R package version 1.4-4.
- 702   Bivand, R., Lewin-Koh, N., 2019. mapproj: Tools for Handling Spatial Objects. R package version 0.9-  
703       5.
- 704   Borcard, D., Gillet, F., Legendre, P., 2011. *Numerical Ecology in R, Use R!* Springer New York  
705       Dordrecht London Heidelberg. <https://doi.org/10.1007/978-1-4419-7976-6>
- 706   Boyd, W.E., Lentfer, C.J., Torrence, R., 1998. Phytolith analysis for wet tropics environment:  
707       methodological issues and implications for the archaeology of garua island, West New Britain,  
708       Papua New Guinea. *Palynology* 22, 213–228.
- 709   Bozarth, S., 1987. Diagnostic Opal Phytoliths from Rinds of Selected Cucurbita Species. *Am. Antiq.*  
710       52, 607–615.
- 711   Bremond, L., Alexandre, A., Hély, C., Guiot, J., 2005. A phytolith index as a proxy of tree cover density  
712       in tropical areas: Calibration with Leaf Area Index along a forest-savanna transect in  
713       southeastern Cameroon. *Glob. Planet. Change*.  
714       <https://doi.org/10.1016/j.gloplacha.2004.09.002>
- 715   Bunting, M.J., Gaillard, M.J., Sugita, S., Middleton, R., Broström, A., 2004. Vegetation structure and  
716       pollen source area. *Holocene* 14, 651–660. <https://doi.org/10.1191/0959683604hl744rp>
- 717   Burbridge, R.E., Mayle, F.E., Killeen, T.J., 2004. Fifty-thousand-year vegetation and climate history of  
718       Noel Kempff Mercado National Park, Bolivian Amazon. *Quat. Res.* 61, 215–230.  
719       <https://doi.org/10.1016/j.yqres.2003.12.004>
- 720   Bush, M.B., Piperno, D.R., Colinvaux, P.A., De Oliveira, P.E., Krissek, L.A., Miller, M.C., Rowe, W.E.,  
721       1992. A 14 300-Yr Paleoecological Profile of a Lowland Tropical Lake in Panama. *Ecol. Monogr.*  
722       62, 251–275. <https://doi.org/10.2307/2937095>
- 723   Butler, D.R., 1995. *Zoogeomorphology : animals as geomorphic agents*. Cambridge University Press.
- 724   Carson, J.F., Mayle, F.E., Whitney, B.S., Iriarte, J., Soto, J.D., 2016. Pre-Columbian ring ditch  
725       construction and land use on a ‘chocolate forest island’ in the Bolivian Amazon. *J. Quat. Sci.* 31,  
726       337–347. <https://doi.org/10.1002/jqs.2835>
- 727   Carson, J.F., Watling, J., Mayle, F.E., Whitney, B.S., Iriarte, J., Prumers, H., Soto, J.D., 2015. Pre-  
728       Columbian land use in the ring-ditch region of the Bolivian Amazon. *The Holocene* 25, 1285–  
729       1300. <https://doi.org/10.1177/0959683615581204>
- 730   Carson, J.F., Whitney, B.S., Mayle, F.E., Iriarte, J., Prumers, H., Soto, J.D., Watling, J., 2014.  
731       Environmental impact of geometric earthwork construction in pre-Columbian Amazonia. *Proc.*  
732       *Natl. Acad. Sci. U. S. A.* 1–6. <https://doi.org/10.1073/pnas.1321770111>

- 733 Clapperton, C.M., 1993. Quaternary Geology and Geomorphology of South America. Elsevier  
734 Science, Amsterdam.
- 735 Colinvaux, P.A., de Oliveira, P.E., Patiño, J.E.M., 1999. Amazon Pollen Manual and Atlas. Harwood  
736 Academic Publishers, Amsterdam.
- 737 Dickau, R., Whitney, B.S., Iriarte, J., Mayle, F.E., Soto, J.D., Metcalfe, P., Street-Perrott, F.A., Loader,  
738 N.J., Ficken, K.J., Killeen, T.J., 2013. Differentiation of neotropical ecosystems by modern soil  
739 phytolith assemblages and its implications for palaeoenvironmental and archaeological  
740 reconstructions. *Rev. Palaeobot. Palynol.* 193, 15–37.  
741 <https://doi.org/10.1016/j.revpalbo.2013.01.004>
- 742 Gabet, E.J., Reichman, O.J., Seabloom, E.W., 2003. The effects of bioturbation on soil processes and  
743 sediment transport. *Annu. Rev. Earth Planet. Sci.* 31, 249–273.  
744 <https://doi.org/10.1146/annurev.earth.31.100901.141314>
- 745 Gosling, W.D., Mayle, F.E., Tate, N.J., Killeen, T.J., 2009. Differentiation between Neotropical  
746 rainforest, dry forest, and savannah ecosystems by their modern pollen spectra and  
747 implications for the fossil pollen record. *Rev. Palaeobot. Palynol.* 153, 70–85.  
748 <https://doi.org/10.1016/j.revpalbo.2008.06.007>
- 749 Gosling, W.D., Mayle, F.E., Tate, N.J., Killeen, T.J., 2005. Modern pollen-rain characteristics of tall  
750 terra firme moist evergreen forest, southern Amazonia. *Quat. Res., Late Quaternary Tropical  
751 Ecosystem Dynamics* 64, 284–297. <https://doi.org/10.1016/j.yqres.2005.08.008>
- 752 Hamilton, S.K., 2002. Hydrological controls of ecological structure and function in the Pantanal  
753 wetland (Brazil), in: *The Ecology of South American Rivers and Wetlands*. IAHS Special  
754 Publication no.6, pp. 133–158.
- 755 Hansen, M.C., Potapov, P. V., Moore, R., Hancher, M., Turubanova, S.A., Tyukavina, A., Thau, D.,  
756 Stehman, S. V., Goetz, S.J., Loveland, T.R., Kommareddy, A., Egorov, A., Chini, L., Justice, C.O.,  
757 Townshend, J.R.G., 2013. High-resolution global maps of 21st-century forest cover change.  
758 *Science* 342, 850–3. <https://doi.org/10.1126/science.1244693>
- 759 Hijmans, R.J., 2019. raster: Geographic Data Analysis and Modeling. R package version 2.9-5.
- 760 Hilbert, L., Góes Neves, E., Pugliese, F., Whitney, B.S., Shock, M., Veasey, E., Augusto Zimpel, C.,  
761 Iriarte, J., 2017. Evidence for mid-Holocene rice domestication in the Americas. *Nat. Ecol. Evol.*  
762 1, 1693–1698. <https://doi.org/10.1038/s41559-017-0322-4>
- 763 Iriarte, J., Paz, E.A., 2009. Phytolith analysis of selected native plants and modern soils from  
764 southeastern Uruguay and its implications for paleoenvironmental and archeological  
765 reconstruction. *Quat. Int.* 193, 99–123. <https://doi.org/10.1016/j.quaint.2007.10.008>
- 766 Jones, H.T., Mayle, F.E., Pennington, R.T., Killeen, T.J., 2011. Characterisation of Bolivian savanna  
767 ecosystems by their modern pollen rain and implications for fossil pollen records. *Rev.  
768 Palaeobot. Palynol.* 164, 223–237. <https://doi.org/10.1016/j.revpalbo.2011.01.001>
- 769 Juggins, S., 2016. C2 Version 1.7: software for ecological and palaeoecological data analysis and  
770 visualisation.
- 771 Julier, A.C.M., Jardine, P.E., Coe, A.L., Gosling, W.D., Lomax, B.H., Fraser, W.T., 2016.  
772 Chemotaxonomy as a tool for interpreting the cryptic diversity of Poaceae pollen. *Rev.  
773 Palaeobot. Palynol.* 235, 140–147. <https://doi.org/10.1016/j.revpalbo.2016.08.004>
- 774 Killeen, T.J., Chavez, E., Pena-Claros, M., Toledo, M., Arroyo, L., Caballero, J., Correa, L., Guillen, R.,  
775 Quevedo, R., Saldias, M., Soria, L., Uslar, Y., Vargas, I., Steininger, M., 2006. The Chiquitano Dry



776 Forest, the Transition Between Humid and Dry Forest in Eastern Lowland Bolivia, in:  
777 Pennington, T.R., Lewis, G.P., Ratter, J.A. (Eds.), Neotropical Savannahs and Seasonally Dry  
778 Forests: Plant Diversity, Biogeography and Conservation. Taylor & Francis, Boca Raton, Florida,  
779 pp. 213–233.

780 Killeen, T.J., Schulenberg, T.S., 1998. A biological assessment of Parc Nacional Noel Kempff Mercado,  
781 Bolivia, RAP Working Papers 10. Conservation International, Washington, DC.

782 Kondo, R., Childs, C., Atkinson, L., 1994. Opal phytoliths of New Zealand. Manaaki Press, Lincoln,  
783 New Zealand.

784 Lu, H., Liu, K.B., 2003. Phytoliths of common grasses in the coastal environments of southeastern  
785 USA. *Estuar. Coast. Shelf Sci.* 58, 587–600. [https://doi.org/10.1016/S0272-7714\(03\)00137-9](https://doi.org/10.1016/S0272-7714(03)00137-9)

786 McGlue, M.M., Silva, A., Zani, H., Corradini, F.A., Parolin, M., Abel, E.J., Cohen, A.S., Assine, M.L., Ellis,  
787 G.S., Trees, M.A., Kuerten, S., Gradella, F. dos S., Rasbold, G.G., 2012. Lacustrine records of  
788 Holocene flood pulse dynamics in the Upper Paraguay River watershed (Pantanal wetlands,  
789 Brazil). *Quat. Res.* 78, 285–294. <https://doi.org/10.1016/j.yqres.2012.05.015>

790 Mercader, J., Bennett, T., Esselmont, C., Simpson, S., Walde, D., 2011. Soil phytoliths from miombo  
791 woodlands in Mozambique. *Quat. Res.* 75, 138–150.  
792 <https://doi.org/10.1016/j.yqres.2010.09.008>

793 Mercader, J., Bennett, T., Esselmont, C., Simpson, S., Walde, D., 2009. Phytoliths in woody plants  
794 from the Miombo woodlands of Mozambique. *Ann. Bot.* 104, 91–113.  
795 <https://doi.org/10.1093/aob/mcp097>

796 Nunes da Cunha, C., Junk, W.J., Leitão Filho, H.D.F., 2007. Woody vegetation in the Pantanal of Mato  
797 Grosso, Brazil: a preliminary typology. *Amazoniana* 19, 159–184.

798 Oksanen, J., Blanchet, F.G., Friendly, M., Kindt, R., Legendre, P., McGlenn, D., Minchin, P.R., O’Hara,  
799 R.B., Simpson, G.L., Solymos, P., Stevens, M.H.H., Szoecs, E., Wagner, H., 2018. vegan:  
800 Community Ecology Package. R package version 2.5-2.

801 Piperno, D.R., 2006. *Phytoliths: A comprehensive guide for Archeologists and Paleoecologists.*  
802 Altamire Press.

803 Piperno, D.R., 1990. Aboriginal agriculture and land usage in the Amazon Basin, Ecuador. *J. Archaeol.*  
804 *Sci.* 17, 665–677. [https://doi.org/10.1016/0305-4403\(90\)90048-A](https://doi.org/10.1016/0305-4403(90)90048-A)

805 Piperno, D.R., 1985. Phytolith analysis and tropical paleo-ecology: Production and taxonomic  
806 significance of siliceous forms in new world plant domesticates and wild species. *Rev.*  
807 *Palaeobot. Palynol.* [https://doi.org/10.1016/0034-6667\(85\)90002-8](https://doi.org/10.1016/0034-6667(85)90002-8)

808 Piperno, D.R., Bush, M.B., Colinvaux, P.A., 1990. Paleoenvironments and human occupation in late-  
809 glacial Panama. *Quat. Res.* 33, 108–116. [https://doi.org/10.1016/0033-5894\(90\)90089-4](https://doi.org/10.1016/0033-5894(90)90089-4)

810 Piperno, D.R., Jones, J.G., 2003. Paleoeological and archaeological implications of a late  
811 Pleistocene/Early holocene record of vegetation and climate from the pacific coastal plain of  
812 panama. *Quat. Res.* 59, 79–87. [https://doi.org/10.1016/S0033-5894\(02\)00021-2](https://doi.org/10.1016/S0033-5894(02)00021-2)

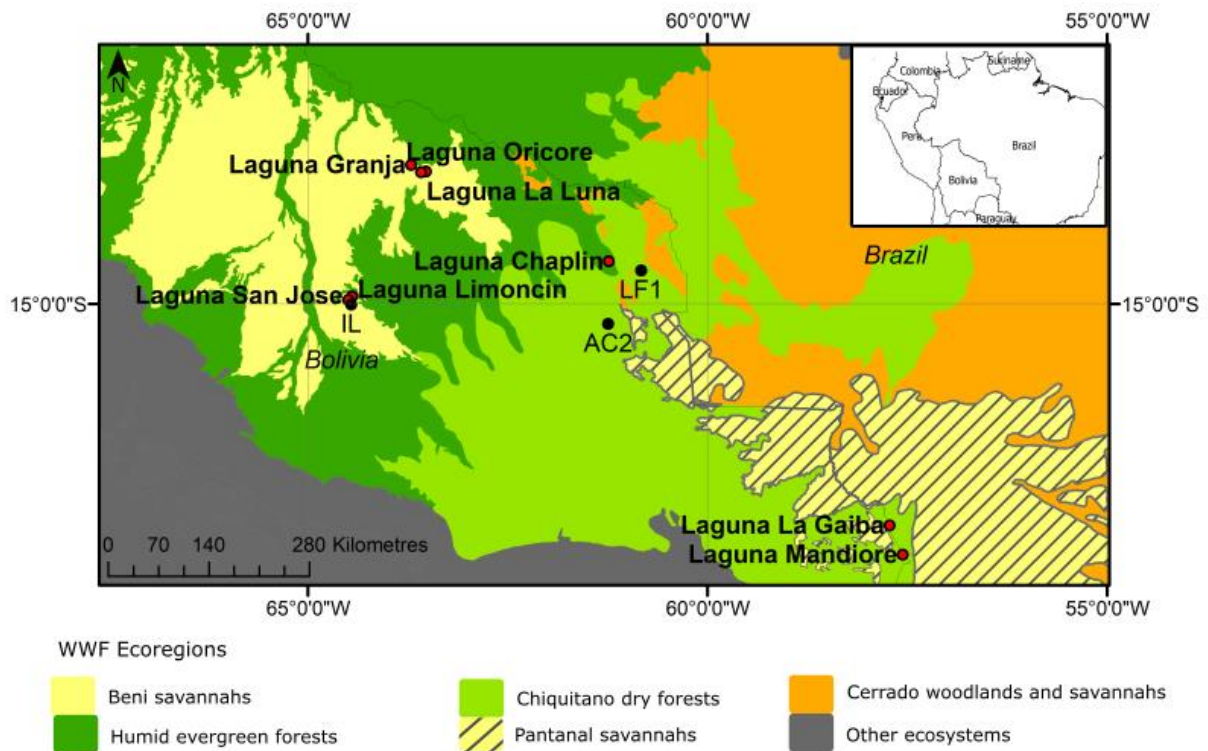
813 Piperno, Dolores R., Pearsall, D.M., 1998. The Silica Bodies of Tropical American Grasses:  
814 Morphology, Taxonomy, and Implications for Grass Systematics and Fossil Phytolith  
815 Identification. *Smithson. Contrib. to Bot.* 1–40. <https://doi.org/10.5479/si.0081024X.85>

816 Piperno, D.R., Pearsall, D.M., 1998. *The Origins of Agriculture in the Lowland Neotropics.* Academic  
817 Press, New York.

- 818 Plumpton, H.J., Mayle, F.M., Whitney B.S., accepted. Long-term impacts of mid-Holocene drier  
819 climatic conditions on Bolivian tropical dry forests. *Quaternary Research*. Accepted 30<sup>th</sup> July  
820 2019.
- 821 Prance, G.T., Schaller, G.B., 1982. Preliminary Study of Some Vegetation Types of the Pantanal, Mato  
822 Grosso, Brazil. *Brittonia* 34, 228. <https://doi.org/10.2307/2806383>
- 823 Rull, V., Montoya, E., 2014. *Mauritia flexuosa* palm swamp communities: Natural or human-made? A  
824 palynological study of the Gran Sabana region (northern South America) within a neotropical  
825 context. *Quat. Sci. Rev.* <https://doi.org/10.1016/j.quascirev.2014.06.007>
- 826 Runge, F., 1999. The opal phytolith inventory of soils in central Africa - Quantities, shapes,  
827 classification, and spectra. *Rev. Palaeobot. Palynol.* 107, 23–53. [https://doi.org/10.1016/S0034-](https://doi.org/10.1016/S0034-6667(99)00018-4)  
828 6667(99)00018-4
- 829 Seiler, C., Hutjes, R.W.A., Kabat, P., Seiler, C., Hutjes, R.W.A., Kabat, P., 2013. Climate Variability and  
830 Trends in Bolivia. *J. Appl. Meteorol. Climatol.* 52, 130–146. [https://doi.org/10.1175/JAMC-D-](https://doi.org/10.1175/JAMC-D-12-0105.1)  
831 12-0105.1
- 832 Sugita, S., 1994. Pollen Representation of Vegetation in Quaternary Sediments: Theory and Method  
833 in Patchy Vegetation. *J. Ecol.* 82, 881–897. <https://doi.org/10.2307/2261452>
- 834 ter Braak, C.J.F., Verdonschot, P.F.M., 1995. Canonical correspondence analysis and related  
835 multivariate methods in aquatic ecology. *Aquat. Sci.* 57, 255–289.  
836 <https://doi.org/10.1007/BF00877430>
- 837 Wallis, L., 2003. An overview of leaf phytolith production patterns in selected northwest Australian  
838 flora. *Rev. Palaeobot. Palynol.* 125, 201–248. [https://doi.org/10.1016/S0034-6667\(03\)00003-4](https://doi.org/10.1016/S0034-6667(03)00003-4)
- 839 Watling, J., Iriarte, J., 2013. Phytoliths from the coastal savannas of French Guiana. *Quat. Int.* 287,  
840 162–180. <https://doi.org/10.1016/j.quaint.2012.10.030>
- 841 Watling, J., Iriarte, J., Mayle, F.E., Schaan, D., Pessenda, L.C.R., Loader, N.J., Street-Perrott, F.A.,  
842 Dickau, R.E., Damasceno, A., Ranzi, A., 2017. Impact of pre-Columbian “geoglyph” builders on  
843 Amazonian forests. *Proc. Natl. Acad. Sci. U. S. A.* 114, 1868–1873.  
844 <https://doi.org/10.1073/pnas.1614359114>
- 845 Watling, J., Iriarte, J., Whitney, B.S., Consuelo, E., Mayle, F.E., Castro, W., Schaan, D., Feldpausch,  
846 T.R., 2016. Differentiation of neotropical ecosystems by modern soil phytolith assemblages and  
847 its implications for palaeoenvironmental and archaeological reconstructions II: Southwestern  
848 Amazonian forests. *Rev. Palaeobot. Palynol.* 226, 30–43.
- 849 Watling, J., Shock, M.P., Mongeló, G.Z., Almeida, F.O., Kater, T., De Oliveira, P.E., Neves, E.G., 2018.  
850 Direct archaeological evidence for Southwestern Amazonia as an early plant domestication and  
851 food production centre. *PLoS One* 13, e0199868.  
852 <https://doi.org/10.1371/journal.pone.0199868>
- 853 Whitney, B.S., Dickau, R., Mayle, F.E., Soto, J.D., Iriarte, J., 2013. Pre-Columbian landscape impact  
854 and agriculture in the Monumental Mound region of the Llanos de Moxos, lowland Bolivia.  
855 *Quat. Res.* 80, 207–217. <https://doi.org/10.1016/j.yqres.2013.06.005>
- 856 Whitney, B.S., Mayle, F.E., Burn, M.J., Guillén, R., Chavez, E., Pennington, R.T., 2014. Sensitivity of  
857 Bolivian seasonally-dry tropical forest to precipitation and temperature changes over glacial–  
858 interglacial timescales. *Veg. Hist. Archaeobot.* 23, 1–14. [https://doi.org/10.1007/s00334-013-](https://doi.org/10.1007/s00334-013-0395-1)  
859 0395-1
- 860 Whitney, B.S., Mayle, F.E., Punyasena, S.W., Fitzpatrick, K.A., Burn, M.J., Guillen, R., Chavez, E.,

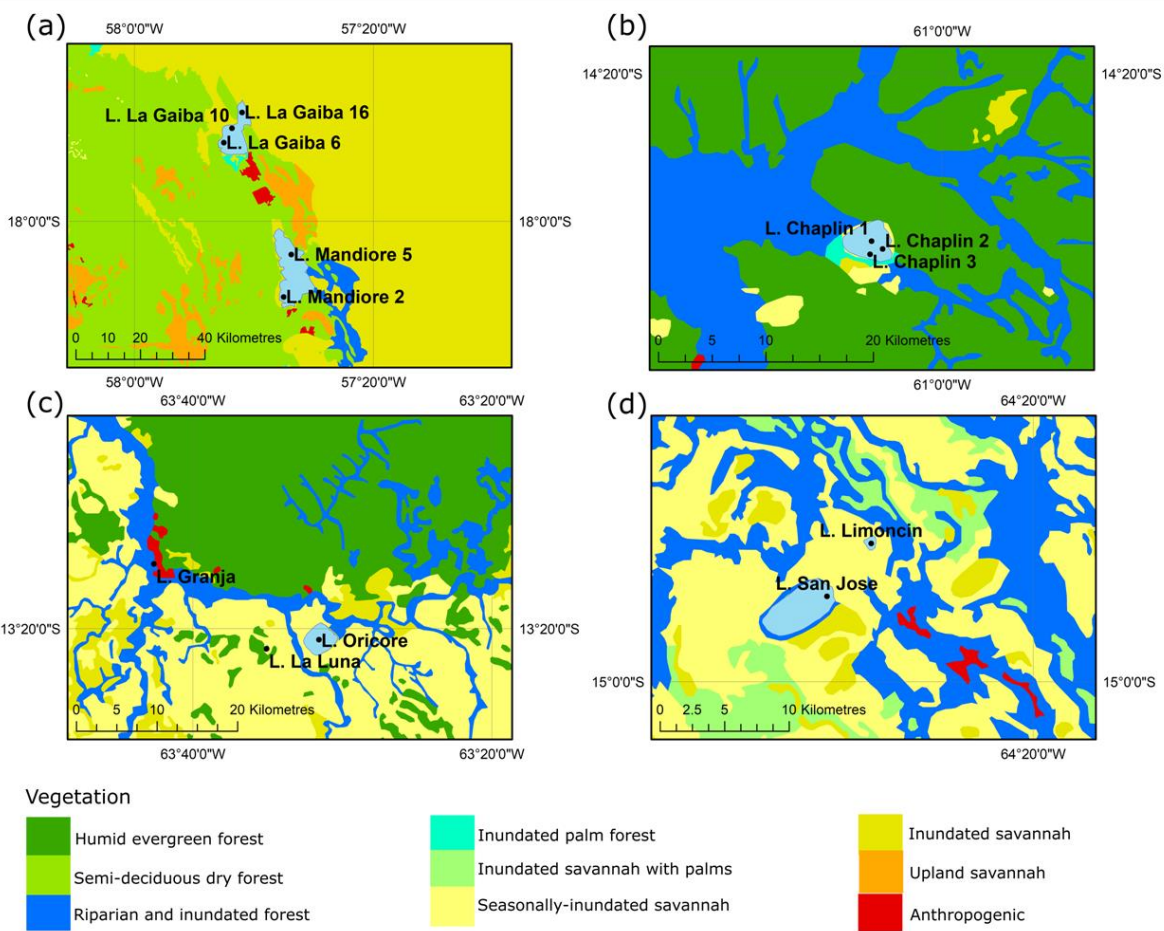
861 Mann, D., Pennington, R.T., Metcalfe, S.E., 2011. A 45kyr palaeoclimate record from the  
862 lowland interior of tropical South America. *Palaeogeogr. Palaeoclimatol. Palaeoecol.* 307, 177–  
863 192. <https://doi.org/10.1016/j.palaeo.2011.05.012>

864 List of Figures



865

866 Figure 1 – Map of lake sites and vegetation surveys plotted against vegetation classifications adapted  
867 from WWF terrestrial ecoregions (Olsen et al 2001) using ArcGIS 10.5.1. Lake sites are shown by red  
868 circles. Vegetation inventories and surveys are shown by black circles (IL = Vegetation survey around  
869 Lagunas Isirere and Limoncin, AC2 = Acuario 2 forest plot inventory, LF1 = Los Fierros 1 forest plot  
870 inventory). Inset map of South America.



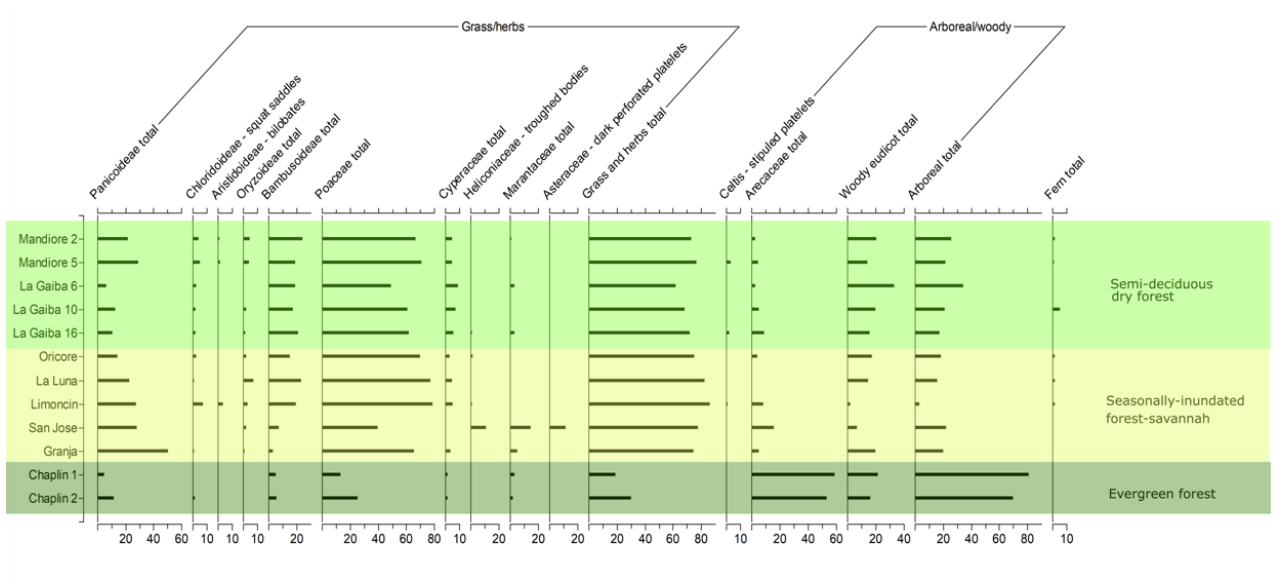
871

872 Figure 2 - Maps of lake sites and surrounding ecosystems created using ArcGIS 10.5.1. Panel A shows  
 873 the Chiquitania-Pantanal study region with Lagunas La Gaiba and Mandioré; Panel B shows terra  
 874 firme humid evergreen forests on the Pre-Cambrian shield study region with Laguna Chaplin; Panel C  
 875 shows the northern areas of the Beni basin study region with Lagunas Oricoré, La Luna and Granja;  
 876 and Panel D shows the southern areas of the Beni basin study region with Lagunas San José and  
 877 Limoncín. The locations of all surface samples are shown for each lake by black circles. Vegetation  
 878 classification of the study area, based on Landsat imagery, was provided by the Museo de Historia  
 879 Natural 'Noel Kempff Mercado', Santa Cruz, Bolivia in 2015. Scale bars and latitude and longitude are  
 880 presented for each individual map panel.

881

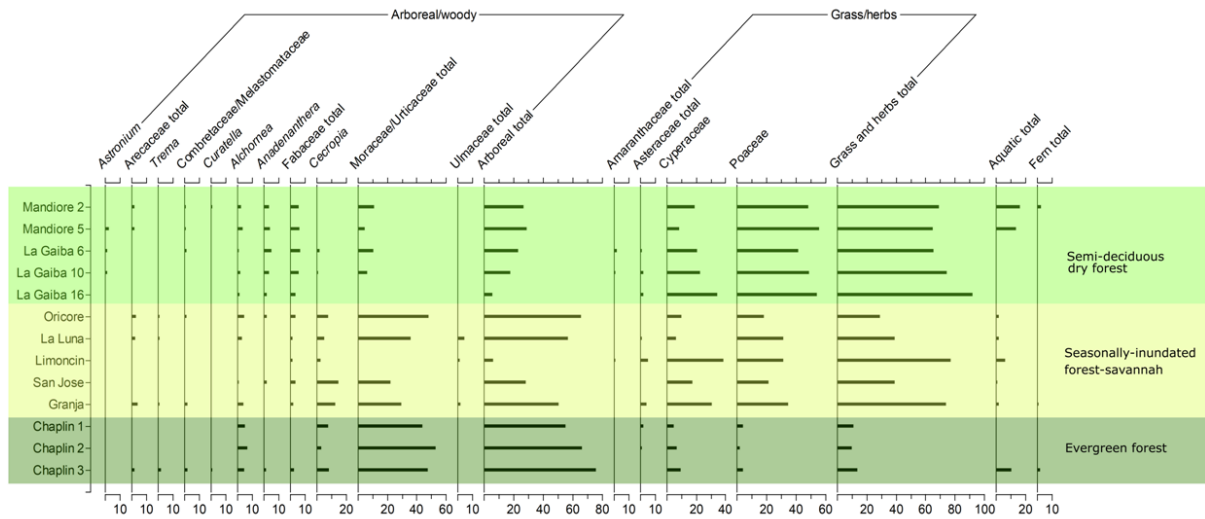
882

883  
 884  
 885  
 886  
 887  
 888



889

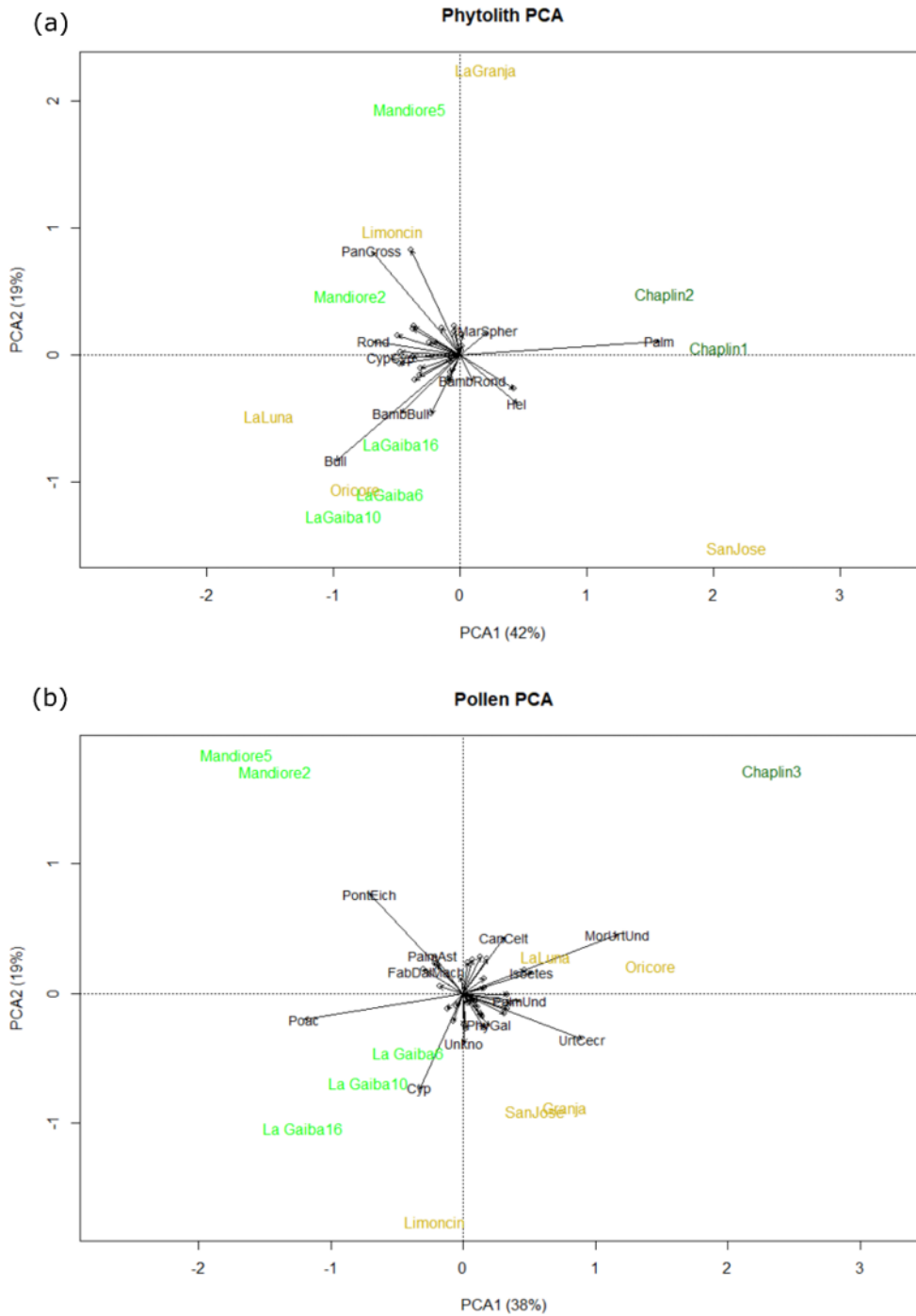
890 Figure 3 – Summary diagram of phytolith abundances from all lakes studied, presented as  
 891 percentage data. Vegetation surrounding the lakes has been classified into 3 ecosystem types: semi-  
 892 deciduous dry forest (Chiquitania-Pantanal), seasonally inundated forest-savannah (Beni basin), and  
 893 evergreen forest (PCS Humid Evergreen Forest).



894

895 Figure 4 – Summary diagram of pollen abundance from all lakes studied, presented as percentage of  
 896 terrestrial total. Vegetation surrounding the lakes has been classified into 3 ecosystem types: semi-  
 897 deciduous dry forest (Chiquitania-Pantanal), seasonally inundated forest-savannah (Beni basin), and  
 898 evergreen forest (PCS Humid Evergreen Forest). Pollen data for Chaplin 1 and 2 is only available in  
 899 highly summarised format with data for a restricted number of taxa. Full pollen counts are available  
 900 for Chaplin 3.

901

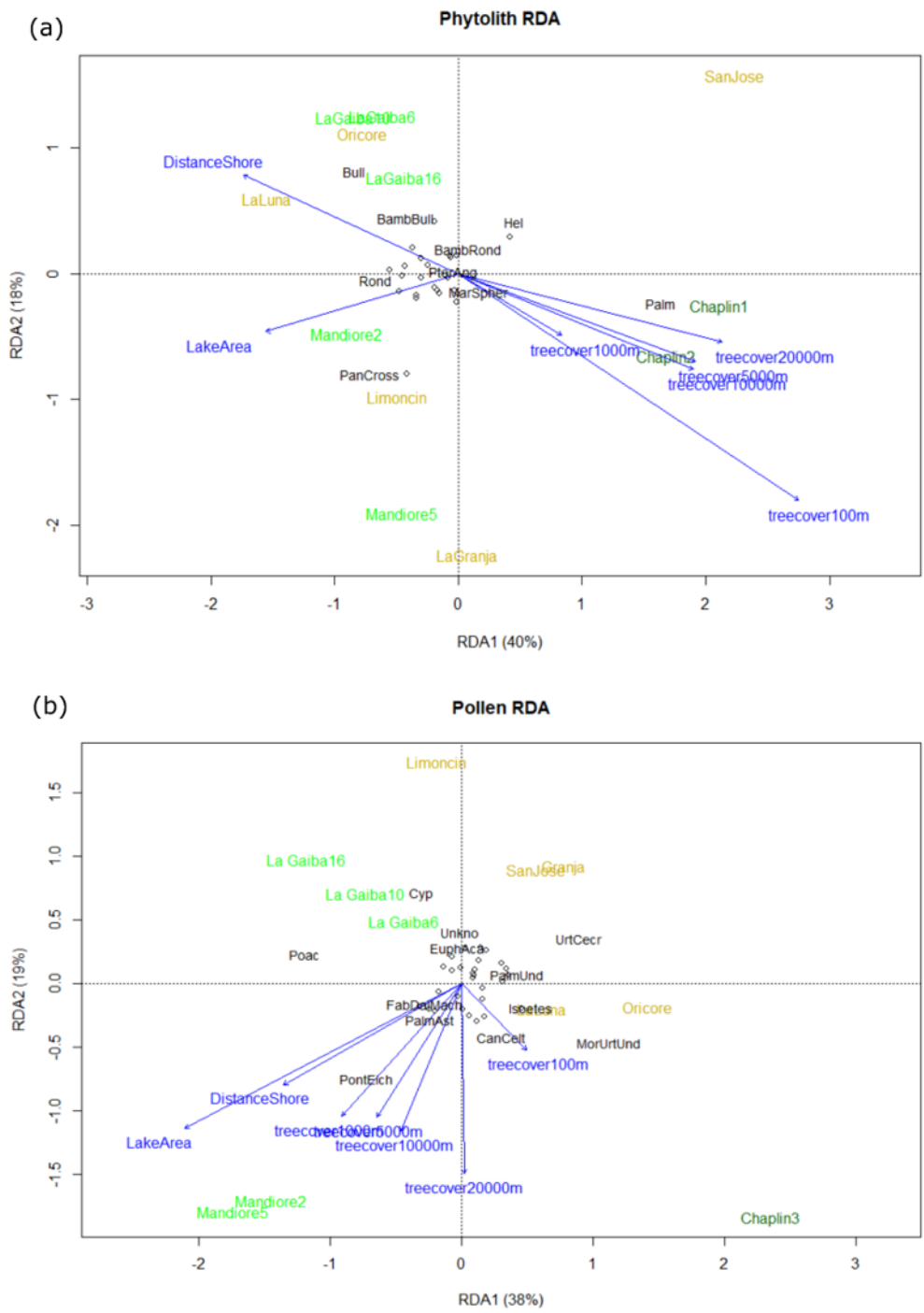


902

903 Figure 5 – PCA biplot for a) phytolith and b) pollen data. Axes are Principal Component 1 (PCA1) and  
 904 Principal Component 2 (PCA2). The percentage in parentheses on these axes is the percentage of  
 905 variance in the dataset explained by that principal component. Lake sites are coloured according to  
 906 the ecosystem they represent: light green = semi-deciduous dry forest, yellow = Beni seasonally-

907 inundated forest-savannah mosaic, dark green = humid evergreen forest. Taxa are presented in  
 908 black. Codes for taxa names are presented in Tables 5 and 6 for phytoliths and pollen respectively.

909



910



911 Figure 6 – RDA tri-plot for a) phytolith and b) pollen data. Axes are Redundancy Analysis 1 (RDA1)  
 912 and 2 (RDA2). The percentage in parentheses on these axes is the percentage of variance in the  
 913 dataset explained by that component. Environmental constraining variables are presented in blue:  
 914 lake area, distance of core site to lake shore, and tree cover within 100, 1000, 2000, 10,000 and  
 915 20,000 m of the lake shore. Lake sites are coloured according to the ecosystem they represent: light  
 916 green = semi-deciduous dry forest, yellow = Beni seasonally-inundated forest-savannah mosaic, dark  
 917 green = humid evergreen forest. Taxa are presented in black. Codes for taxa names are presented in  
 918 Tables 5 and 6 for phytoliths and pollen respectively.

919

920 List of Tables

921 Table 1 - Summary of lake site characteristics, including references to the papers originally publishing  
 922 some of the pollen and phytolith records.

Lake	No. samples	Region	Ecosystem	Area of lake /km <sup>2</sup>	Pollen analysed by	Phytoliths analysed by
<b>Mandioré</b>	2	Chiquitania-Pantanal	Semi-deciduous forest/Pantanal wetlands	152	Plumpton et al., accepted	Plumpton et al., accepted
<b>La Gaiba</b>	3	Chiquitania-Pantanal	Semi-deciduous forest/Pantanal wetlands	90	Whitney et al., 2011	Plumpton et al., accepted
<b>Oricoré</b>	1	Beni Basin	Seasonally-inundated savannah-forest mosaic	10.5	Carson et al., 2014	<i>This study</i>
<b>La Luna</b>	1	Beni Basin	Seasonally-inundated savannah-forest mosaic	0.33	Carson et al., 2016	<i>This study</i>
<b>Limoncín</b>	1	Beni Basin	Seasonally-inundated savannah-forest mosaic	0.73	<i>Whitney, unpublished</i>	<i>This study</i>

<b>San José</b>	1	Beni Basin	Seasonally-inundated savannah-forest mosaic	14.3	Whitney et al., 2013	Whitney et al., 2013
<b>Granja</b>	1	Beni basin/ Terra firme evergreen forest on PCS	Seasonally-inundated savannah-forest mosaic /Terra firme evergreen forest	0.071	Carson et al., 2015	Carson et al., 2015
<b>Chaplin</b>	2	Terra firme evergreen forest on PCS	Terra firme evergreen forest	12.2	Burbridge et al., 2004	<i>This study</i>

923

924

925

926 Table 2 – Vegetation inventory of Acuario 2, a 1-hectare vegetation plot within Noel Kempff

927 Mercado National Park, gives a representative vegetation community composition for semi-

928 deciduous dry forest in south-west Amazonia. Inventory conducted by recording all taxa

929 representing >1% of the total number of stems >10cm d.b.h. (Gosling et al., 2009).

<b>Family</b>	<b>Species</b>	<b>% of total stems</b>
Fabaceae — Caes.	<i>Caesalpinia floribunda</i> Tul.	11.72
Bignoniaceae	<i>Tabebuia roseo-alba</i> (Ridley) Sandwith	7.42
Fabaceae — Mim.	<i>Anadenanthera colubrina</i> (Vell.) Brenan	7.03
Flacourtiaceae	<i>Casearia gossypiosperma</i> Brig.	6.25
Combretaceae	<i>Combretum leprosum</i> Mart.	5.66
Arecaceae	<i>Orbignya phalerata</i> Mart.	3.71
Fabaceae — Caes.	<i>Bauhinia rufa</i> (Bong.) Steud.	3.32
Rubiaceae	<i>Simira cordifolia</i> (Hook. f.) Steyerm.	2.93
Boraginaceae	<i>Cordia alliodora</i> (Ruíz and Pavón) Oken	2.73
Sterculiaceae	<i>Guazuma ulmifolia</i> Lam.	2.73
Apocynaceae	<i>Aspidosperma cylindrocarpon</i> Müll. Arg.	2.34
Sterculiaceae	<i>Sterculia apetala</i> (Jacq.) Karsten	2.15
Flacourtiaceae	<i>Casearia arborea</i> (Rich.) Urban	1.95
Rhamnaceae	<i>Rhamnidium elaeocarpum</i> Reisseck	1.95
Arecaceae	<i>Scheelea princeps</i> (Mart.) Karsten	1.76
Malvaceae	<i>Chorisia integrifolia</i> Ulbr.	1.76
Meliaceae	<i>Cedrela fissilis</i> Vell.	1.76

Sapindaceae	<i>Dilodendron bipinnatum</i> Radlk.	1.76
Anacardiaceae	<i>Spondias mombin</i> L.	1.56
Bignoniaceae	<i>Arrabidaea spicata</i> Bureau and K. Schum	1.37
Euphorbiaceae	<i>Sebastiania huallagensis</i> Croizat	1.37
Tiliaceae	<i>Apeiba tibourbou</i> Aubl.	1.37
Malvaceae	<i>Pseudobombax marginatum</i> (A. St.-Hil.) Robyns	1.17
Fabaceae — Pap.	<i>Machaerium villosum</i> Vogel	1.17
Malpighiaceae	<i>Dicella macroptera</i> A. Juss.	1.17
Fabaceae — Pap.	<i>Machaerium acutifolium</i> Vogel	0.98
Tiliaceae	<i>Triumfetta grandiflora</i> Vahl	0.98
<b>TOTAL</b>		<b>80.08</b>

930

931 Table 3 – Results of a qualitative vegetation survey ranking taxa as dominant, abundant, frequent or  
932 occasional in coverage from the area surrounding Lagunas Limoncin and Isirere are presented to give  
933 an example vegetation community composition for the Beni seasonally-inundated savannah. (Dickau  
934 et al., 2013).

Family	Species	Abundance classification (Soto 2010)
Marantaceae	<i>Thalia geniculata</i>	Dominant (>50%)
Fabaceae	<i>Inga stenopoda</i>	Dominant (>50%)
Fabaceae	<i>Erythrina fusca</i>	Abundant (20-50%)
Cyperaceae	<i>Cyperus gigantus</i>	Abundant (20-50%)
Heliconiaceae	<i>Heliconia sp.</i>	Abundant (20-50%)
Typhaceae	<i>Typha domingensis</i>	Frequent (10-20%)
Moraceae	<i>Ficus sp.</i>	Frequent (10-20%)
Cannaceae	<i>Canna glauca</i>	Occasional (2-10%)
Urticaceae	<i>Cecropia sp.</i>	Occasional (2-10%)

935

936 Table 4 – Vegetation inventory of Los Fierros 1, a 1-hectare vegetation plot within Noel Kempff  
937 Mercado National Park, gives a representative vegetation community composition for evergreen  
938 forest in south-west Amazonia. Inventory conducted by recording all taxa representing >1% of the  
939 total number of stems >10cm d.b.h. (Gosling et al., 2005).

Family	Species	% of total stems
Strelitziaceae	<i>Phenakospermum guianensis</i> Aubl.	13.07
Moraceae	<i>Pseudolmedia laevis</i> (Ruiz and Pav.) J. F. Macbr.	7.64

Arecaceae	<i>Euterpe precatoria</i> Mart.	6.91
Rubiaceae	<i>Capirona decorticans</i> Spruce	6.29
Vochysiaceae	<i>Qualea paraenesis</i> Ducke	6.04
Vochysiaceae	<i>Erisma uncinatum</i> Warm.	4.19
Elaeocarpaceae	<i>Sloanea eichleri</i> K. Schum.	3.45
Moraceae	<i>Pseudolmedia macrophylla</i> Trécul	3.33
Rubiaceae	<i>Amaioua guianensis</i> Aubl.	3.08
Hippocrateaceae	<i>Cheiloclinium cognatum</i> (Miers) A. C. Sm.	2.84
Euphorbiaceae	<i>Hyeronima oblonga</i> (Tul.) Müll. Arg.	2.47
Arecaceae	<i>Socratea exorrhiza</i> (Mart.) H. L. Wendl.	2.1
Moraceae	<i>Pourouma guianensis</i> Aubl.	1.85
Melastomataceae	<i>Miconia pyrifolia</i> Naudin	1.6
Moraceae	<i>Brosimum acutifolium</i> subsp. <i>obovatum</i> (Ducke) C. C. Berg.	1.6
Lythraceae	<i>Physocalymma scaberrimum</i> Pohl	1.11
Melastomataceae	indet. 3	1.11
Lauraceae	<i>Nectandra</i> sp. 2	0.99
Melastomataceae	<i>Miconia multiflora</i> Cogn.	0.99
Melastomataceae	<i>Miconia</i> sp. 3	0.99
Moraceae	<i>Helicostylis tomentosa</i> (Poepp. and Endl.) Rusby	0.99
<b>TOTAL</b>		<b>72.63</b>

940

941 Table 5 – Phytoliths types identified with abundance >1%, their taxonomic association and PCA/RDA  
942 codes.

Phytolith type	Association	References	PCA/RDA code
Bilobates	Panicoideae	1–6	PanBilob
Polylobates	Panicoideae	1–6	PanPolyb
Crosses	Panicoideae	5–12	PanCross
Squat saddles	Chloridoideae	2, 3, 5, 6, 13	Chloro
Aristida bilobates	Aristidoideae	5, 6	Arist
Rondels	Poaceae	2, 3, 5, 6	Rond
Rondeloid/saddeloid	Bambusoideae	5	BambRond
Collapsed saddles	Bambusoideae	5–7, 14, 15	BambCSaddle
Tall saddles	Bambusoideae	6	BambTSaddle
Bilobates (blocky)	Bambusoideae	6	BambBilob
Crosses (blocky)	Bambusoideae	5–12	BambCross
Chusquoid bodies	Bambusoideae	5, 6	BambChusquoid
Two-spiked crown bodies	Bambusoideae	5	BambCrown
Chusquea bodies	Bambusoideae	5, 6	BambChusquea
Oryzae scooped bilobates	Oryzae	1, 16	OryzBilob
Oryzae scooped crosses	Oryzae	1, 16	OryzCross
Olyreae bodies	Olyreae	5, 17	BambOlyra
Bulliforms	Poaceae	6, 7	Bull

Bulliforms (bamb)	Bambusoideae	35	BambBull
Cyperaceae cones	Cyperaceae	13, 20–23	CypCone
Scirpus achene	Cyperaceae	20	CypScir
Cyperus/Carex achene	Cyperaceae	20	CypCyp
<i>Heliconia</i> troughed body	<i>Heliconia</i>	6, 18, 19	Hel
Marantaceae globular nodular	Marantaceae	23	MarSpher
Marantaceae seed	Marantaceae	23	MarSeed
Strelitziaceae druse	Strelitziaceae	18	Strel
Echinate globular/hat	Arecaceae	6, 13, 17, 18, 24, 25	Palm
Echinate irregular platelet	<i>Celtis</i>	17, 28	Celtis
Globular granulate	Woody eudicot	6, 26, 27	GlobGran
Faceted elongate	Woody eudicot	6	Arbor
Terminal tracheid	Woody eudicot	6, 7	TermTrach
Asteraceae platelets	Asteraceae	6, 7, 32	Ast
Vesicular infillings	Woody eudicot	29, 30	VesFill
Scooped globular	Pteridophyte, <i>Trichomanes</i>	31	PterGlob

943 References: 1. (Metcalf 1960); 2. (Twiss et al. 1969); 3. (Brown 1984); 4. (Fredlund & Tieszen 1994);  
944 5. (Piperno & Pearsall 1998); 6. (Piperno 2006); 7. (Piperno 1988); 8. (Piperno 1984); 9. (Pearsall  
945 1978); 10. (Pearsall 1982); 11. (Pearsall & Piperno 1990); 12. (Iriarte 2003); 13. (Kondo et al. 1994);  
946 14. (Lu 1995); 15. (Lu et al. 2006); 16. (Chaffey 1983); 17. (Watling & Iriarte 2013); 18. (Tomlinson  
947 1961); 19. (Prychid et al. 2003); 20. (Ollendorf 1992); 21. (Honaine et al. 2009); 22. (Metcalf 1971);  
948 23. (Wallis 2003); 24. (Runge 1999); 25. (Bozarth et al. 2009); 26. (Amos 1952); 27. (Scurfield et al.  
949 1974); 28. (Bozarth 1992); 29. (Stromberg 2003); 30. (Strömberg 2004); 31. (Mazumdar 2011).

950 Table 6 – Pollen taxa identified with abundance >1% and PCA/RDA codes.

Family	Genus or species	PCA/RDA code
Amaranthaceae	<i>Alternanthera</i>	AmarAlt
Amaranthaceae	<i>Amaranthus/Chenopodiaceae</i>	AmarAma
Amaranthaceae	<i>Gomphrena</i>	AmarGom
Anacardiaceae	<i>Astronium</i>	AnacAst
Anacardiaceae	<i>Schinopsis</i>	AnacSch
Anacardiaceae	<i>Spondias</i>	AnacSpo
Anacardiaceae	<i>Tapirira</i>	AnacTap
Annonaceae	<i>Annona</i>	AnnonAnn
Apocynaceae	<i>Prestonia</i>	ApoPres
Araliaceae	<i>Didymopanax</i>	AralDid
Arecaceae	undiff.	PalmUnd

---

Arecaceae	<i>Astrocaryum</i>	PalmAst
Arecaceae	<i>Copernicia</i>	PalmCop
Arecaceae	<i>Mauritia</i>	PalmMaur
Arecaceae	<i>Sygarus</i>	PalmSyg
Asteraceae	<i>Mikania</i> -type	AstMik
Asteraceae	undiff.	AstUnd
Asteraceae	<i>Ambrosia</i> -type	AstAmb
Bignoniaceae	<i>Jacaranda</i>	BigJac
Bromeliaceae	undiff.	Brom
Burseraceae	<i>Bursera</i> -type	BurBurs
Cannabaceae	<i>Celtis</i>	CanCelt
Cannabaceae	<i>Trema</i>	CanTrem
Combretaceae/Melastomataceae	undiff.	CombMelUnd
Melastomataceae	<i>Miconia</i>	CombMelMic
Cyperaceae	undiff.	Cyp
Dilleniaceae	<i>Curatella americana</i>	DillCur
Erythroxylaceae	<i>Erthroxylum</i>	EryEryth
Euphorbiaceae	<i>Acalypha</i>	EuphAca
Euphorbiaceae	<i>Alchornea</i>	EuphAlch
Euphorbiaceae	<i>Hura</i> -type	EuphHura
Euphorbiaceae	<i>Sapium</i>	EuphSap
Euphorbiaceae	<i>Asparisthium</i>	EuphAsp
Fabaceae	<i>Copaifera</i>	FabCopa
Fabaceae	<i>Macrolobium</i>	FabMacr
Fabaceae	<i>Apuleia leiocarpa</i>	FabApul
Fabaceae	<i>Dalbergia/Macherium</i>	FabDalMach
Fabaceae	<i>Erythrina</i>	FabEryth
Fabaceae	<i>Senna</i> -type	FabSen
Fabaceae	undiff.	FabUnd
Fabaceae	<i>Acacia</i>	FabAcac
Fabaceae	<i>Anadenanthera</i>	FabAnad
Fabaceae	<i>Inga</i>	FabInga
Fabaceae	<i>Mimosa</i>	FabMimo
Lamiaceae	<i>Hyptis</i>	LamHyp
Lamiaceae	<i>Vitex</i> -type	LamVit
Malpighiaceae	<i>Byrsonima</i>	MalpBrys
Malpighiaceae	"periporate"	MalpPeri
Malvaceae	<i>Bytternia</i> -type	MalvBytt
Malvaceae	undiff.	MalvUnd
Malvaceae	<i>Guazuma</i> -type	MalvGuaz
Meliaceae	<i>Cedrela/Trichilia</i>	MeliCedTri
Moraceae/Urticaceae	undiff.	MorUrtUnd
Moraceae	<i>Brosimum</i>	MorBros
Moraceae	<i>Ficus</i>	MorFic
Moraceae	<i>Helicostylis</i>	MorHeli
Moraceae	<i>Maclura</i>	MorMacl

---

---

Moraceae	<i>Maquira</i>	MorMaq
Moraceae/Urticaceae	<i>Pourouma/Sorocea</i>	MorUrtPourSor
Moraceae	<i>Pseudolmedia</i>	MorPsued
Urticaceae	<i>Cecropia</i>	UrtCecr
Myrtaceae	undiff.	Myrt
Phytolaccaceae	<i>Gallesia</i>	PhyGal
Phyllanthaceae	<i>Amanoa</i>	PhylAma
Piperaceae	<i>Piper</i>	PipPiper
Poaceae	undiff.	Poac
Polygonaceae	<i>Symmeria</i>	PolySym
Polygonaceae	<i>Triplaris</i>	PolyTrip
Rubiaceae	<i>Borreria</i> "pericolporate"	RubBorrPeri
Rubiaceae	<i>Borreria latifolia</i>	RubBorrLat
Rubiaceae	<i>Borreria</i> "undiff."	RubBorrUnd
Rubiaceae	<i>Faramea</i>	RubFar
Rubiaceae	<i>Uncaria</i>	RubUnc
Rubiaceae	undiff.	RubUnd
Saliaceae	undiff.	Sali
Sapindaceae	undiff.	SapinUnd
Sapindaceae	<i>Dilodendron</i>	SapinDilo
Sapindaceae	<i>Talisia</i>	SapinTal
Sapotaceae/Melastomataceae	undiff.	SapotMel
Sapotaceae	<i>Pouteria</i>	SapotPout
Solanaceae	undiff.	Solan
Ulmaceae	<i>Ampeloera</i> -type	UlmAmp
Ulmaceae	<i>Phyllostylon</i>	UlmPhyll
Vitaceae	<i>Cissus</i>	VitCis
Vochysiaceae	<i>Vochysia</i>	VocVochy
"Unknowns"	"Unknowns"	Unkno
Alismataceae	<i>Sagittaria</i>	AlisSagg
Alismataceae	<i>Echinodorus</i>	AlisEchin
Pontederiaceae	<i>Eichhornia</i>	PontEich
Polygonaceae	<i>Polygonum</i>	PolyPolyg
Selaginellaceae	<i>Selaginella</i>	SelSelag
Typhaceae	<i>Typha</i>	TypTypha
Isoetes	undiff.	Isoetes
Onagraceae	<i>Ludwigia</i>	OnagLud
Fern	Parkeriaceae	PterPark
Fern	<i>Polypodium</i>	PterPoly

---

951

952 [Supplementary Information](#)

953 S1 – Results of permutation test on RDA results for pollen.

```

954 Permutation test for rda under reduced model
955 Terms added sequentially (first to last)
956 Permutation: free
957 Number of permutations: 999
958
959 Model: rda(formula = pollen.trim.sq ~ LakeArea + DistanceShore + treecover
960 100m + treecover1000m + treecover5000m + treecover10000m + treecover20000m
961 , data = pollen.env)
962
963      Df Variance      F Pr(>F)
964 LakeArea      1  7.8826 11.6825 0.001 ***
965 DistanceShore 1  1.4076  2.0861 0.067 .
966 treecover100m 1  3.2239  4.7780 0.001 ***
967 treecover1000m 1  1.6132  2.3909 0.043 *
968 treecover5000m 1  1.8427  2.7309 0.035 *
969 treecover10000m 1  2.2946  3.4007 0.015 *
970 treecover20000m 1  4.8210  7.1450 0.001 ***
971 Residual      3  2.0242
972 ---
973 Signif. codes:  0 '***' 0.001 '**' 0.01 '*' 0.05 '.' 0.1 ' ' 1

```

974 S2 – Results of permutation test on RDA results for phytoliths.

```

975 Permutation test for rda under reduced model
976 Terms added sequentially (first to last)
977 Permutation: free
978 Number of permutations: 999
979
980 Model: rda(formula = phyto.trim.sq ~ LakeArea + DistanceShore + treecover1
981 00m + treecover1000m + treecover5000m + treecover10000m + treecover20000m,
982 data = phyto.env)
983
984      Df Variance      F Pr(>F)
985 LakeArea      1  2.6529  2.4699 0.059 .
986 DistanceShore 1  2.5158  2.3422 0.063 .
987 treecover100m 1  6.1033  5.6822 0.001 ***
988 treecover1000m 1  2.3299  2.1692 0.059 .
989 treecover5000m 1  4.9024  4.5642 0.003 **
990 treecover10000m 1  2.1535  2.0050 0.098 .
991 treecover20000m 1  1.5547  1.4474 0.201
992 Residual      4  4.2964
993 ---
994 Signif. codes:  0 '***' 0.001 '**' 0.01 '*' 0.05 '.' 0.1 ' ' 1

```

995